

Global MHD Eigenmodes of the Outer Magnetosphere

Andrew N. Wright

Mathematical Institute, University of St. Andrews, St. Andrews, Fife, U.K.

Ian R. Mann

Department of Physics, University of Alberta, Edmonton, Alberta, Canada

In this review we concentrate on the behavior of Ultra-Low Frequency (ULF) Pc5 waves in the terrestrial magnetosphere, including the dayside, flanks, and magnetotail. Theory allows us to predict how the waves are excited, couple from one mode to another, and are damped. The details depend upon the equilibrium in which the waves exist, and have led to the development of “magnetospheric seismology” which compares the predictions of theory with observations. Throughout this article we show how observations and theory can give a remarkably consistent picture of the ULF waves in the magnetosphere, and the underlying structure of the magnetosphere itself. It is also demonstrated how the global nature of magneto-hydrodynamic (MHD) waves brings together traditionally diverse and separate areas of study such as magnetopause stability, magnetosphere-ionosphere coupling, substorms, current circuits, and auroral arc formation as different aspects of a unified view of the dynamic magnetosphere.

1. INTRODUCTION

The global scale time-dependent behavior of the magnetosphere is naturally described in terms of MHD waves. As these waves propagate they transport energy throughout the system, couple different regions together and form part of the magnetospheric current circuit. Theory and observations of ULF waves have a tradition of developing together and provide much insight and understanding of the magnetosphere. A historical review is given by *Hughes* [1994]. The origins of theory date back to *Dungey's* [1954; 1967] consideration of MHD waves in a cold axisymmetric magnetic field. In this case only the fast and Alfvén modes exist, and were shown to decouple when the

waves fields are axisymmetric (i.e., the azimuthal wavenumber $m = 0$).

The Alfvén mode is analogous to a wave on a nonuniform string, and transports energy strictly along the background field direction, as well as a field-aligned current (FAC) carried by electron motion. The fast mode is somewhat similar to a sound wave, and is able to propagate and transport energy isotropically. The decoupled fast mode is similar to a radial “breathing” motion of the magnetosphere, whereas the decoupled (toroidal) Alfvén wave is similar to an axisymmetric twisting motion of the entire L -shell. Often the latter are standing waves having nodes of displacement in the ionosphere. (There also exists a large- m poloidal Alfvén mode—see *Radoski* [1967].) Further properties of these modes and their polarizations are described in the review by *Wright* [1994].

For small azimuthal wavenumbers the (toroidal) Alfvén modes are coupled to the fast mode, but the decoupled modes can yield considerable insight and can provide the leading order solution. *Dungey* [1954; 1967] showed how the Alfvén waves on each L -shell were decoupled from

one another, and so a set of natural Alfvén frequencies $\omega_A(L)$ can be defined for each L -shell. If the fast mode has a coherent oscillation, special field lines exist where the fast mode frequency matches the Alfvén frequency $\omega_A(L)$ and efficient energy transfer from the fast mode to the Alfvén mode can occur via a process known as field line resonance (FLR). This was originally solved for the “box” model magnetosphere [Southwood, 1974] who showed the presence of a singularity in the wave fields at the resonant field line. Chen and Hasegawa [1974] considered a similar situation, but for a dipole magnetic field geometry. By considering the equilibrium field lines to be locally straight they also found the resonant singularity, which has subsequently been demonstrated in more general magnetic geometries [see Wright and Thompson, 1994, and references therein].

The coupling process is analogous to the excitation of a simple harmonic oscillator, the driven localised discrete frequency Alfvén waves showing an amplitude maximum and a 180° phase change with latitude across the resonant field line [Southwood, 1974; Chen and Hasegawa, 1974]. The fast-Alfvén wave coupling in these FLRs can be very efficient in the low- m regime, the strongest coupling occurring for $m \sim 3$ [e.g., Allan et al., 1986a; Kivelson and Southwood, 1986; Zhu and Kivelson, 1988]. As we shall see in this article, the picture described above has been developed extensively over the last two decades to accommodate observations of ULF waves in magnetospheric waveguides, wave coupling on open field lines, and auroral electron acceleration.

Section 2 focuses on the traditional closed “cavity” model of the magnetosphere. Section 3 examines the excitation, character, and ULF wave modes supported by the dayside/flank waveguide including the FLRs driven by outer magnetospheric waveguide modes. Section 4 examines the waves supported by the nightside magnetotail waveguide and the dynamics of mode coupling, relating the wave characteristics to auroral arc signatures. Note that these field lines are (effectively) “open” and the details of mode coupling are different to those on closed field lines. Section 5 examines finite perpendicular scale Alfvén waves carrying intense FACs, and examines the relationship between ULF wave fields and the acceleration of auroral electrons. Finally, section 6 summarises and concludes our review.

2. FIELD LINE RESONANCES AND CAVITY MODES

2.1. Discrete Frequency Field-Line Resonances

On the dayside, early ground-based magnetometer observations of magnetic pulsations in the Pc5 band by Samson et al., [1971] showed polarisation was characterised by propagation

away from noon down both flanks. An amplitude maximum, polarisation reversal, and 180° phase change with latitude were also observed, being later explained by field-line resonance (FLR) theory [see also Walker et al., 1979]. This tied the FLR excitation to a solar wind source, but since discrete frequency FLRs were observed a mechanism was required to generate preferred oscillation frequencies in the magnetosphere.

Early suggestions [Southwood, 1974; Chen and Hasegawa, 1974] proposed a Kelvin-Helmholtz (K.-H.) surface wave driver, and studies such as that by Walker [1981] demonstrated how a finite width magnetopause velocity shear layer can generate a somewhat broad peak in linear growth rate as a function of azimuthal (down-tail) wavelength ($k_{y,max} d \sim 0.6$, where d is the half-width of the velocity shear-layer). This translates to wave periods $T \sim 10d/V_0$, where $2V_0$ is the velocity shear. To produce reasonable periods (320 s) requires a rather thick low latitude boundary layer (LLBL) ($1R_E$) and slow flow (200 km/s), but this corresponds to a somewhat larger azimuthal wavenumber ($m \approx 15$) than is observed.

Most FLRs have a low m value (≈ 4), mHz frequencies and a distinct amplitude peak that is localized in L -shell [e.g., Samson et al., 1971; 1991a; 1991b; 1992a; 1992b; Walker et al., 1992]. These studies showed two or more FLRs (with different frequencies and L -shells) can exist simultaneously, and indicate that the K.-H. surface wave cannot be the only energy source. Figure 1, taken from Mathie and Mann, [2000a], shows the structure of Pc5 ULF wave pulsations in the H-component (magnetic north-south) from the IMAGE ground-based magnetometer array [Lühr, 1994] in the morning local time sector during a fast solar wind speed interval (~ 750 km/s as observed by IMP8). Figure 2 shows the frequency spectra between 0610UT and 0810UT for the data in Figure 1, verifying the existence of multiple, latitude-independent discrete spectral peaks.

Figure 3, also taken from Mathie and Mann [2000a], shows another example of discrete frequency FLRs. The amplitude and phase structure of 4 discrete frequency pulsations are shown as a function of latitude, again as measured by the IMAGE array. The expected FLR amplitude peak and phase change with latitude are apparent in the figure; lower discrete frequency amplitude peaks occur at a higher latitudes as expected for an Alfvén continuum whose frequency decreases with increasing L .

Observations such as these can be explained by cavity mode theory [Kivelson et al., 1984]. Discrete fast compressional modes are trapped between a wave turning point inside the magnetosphere and an outer reflecting boundary such as the magnetopause [Kivelson and Southwood, 1985; 1986], or alternatively the bow shock, [e.g., Harrold and Samson, 1992]. In this model, the natural frequencies of the magnetospheric cavity determine the spectral structure of the discrete fast modes and hence the discrete frequencies of the resulting driven FLRs.

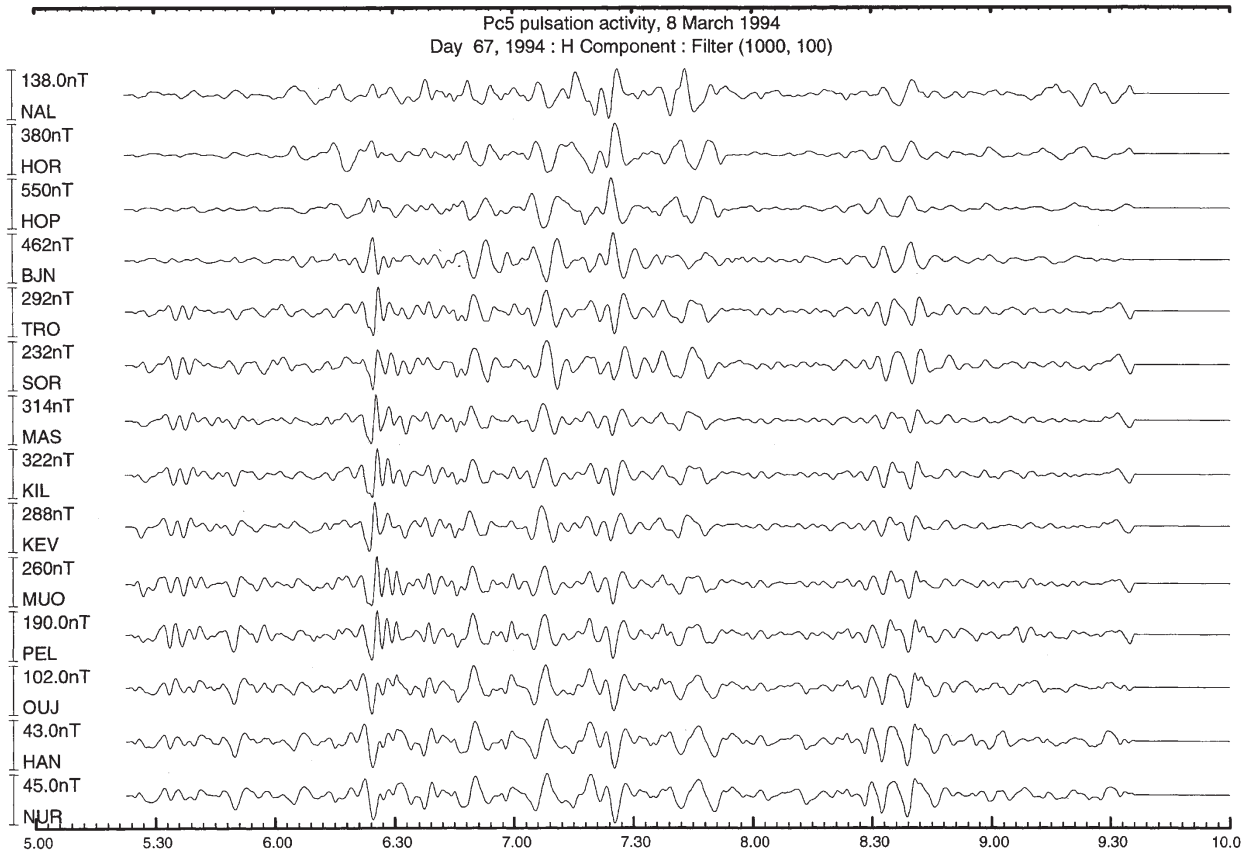


Figure 1. H-component ground-based magnetometer time-series from selected stations in the IMAGE array from March 8th 1994. Time-series as a function of UT are stacked in order of decreasing latitude, and the data have been band-pass filtered between 100s and 1000s period (taken from *Mathie and Mann [2000a]*).

2.2. Magnetospheric Cavity Modes

The cavity model offered an explanation for the multiple discrete frequency harmonic FLRs often observed in the outer magnetosphere. Analysis of the discrete frequencies of the FLRs resulted in the remarkable observation that there appears to be a preferred set of discrete FLR frequencies in the mHz range (1.3, 1.9, 2.6, 3.4 mHz) with remarkable temporal stability and recurrence [see e.g., *Samson et al., 1991a; 1992a; Walker et al., 1992; Ruohoniemi et al., 1991*]. Later studies showed that whilst frequencies such as these were common, not all FLRs were observed with these discrete frequencies [*Fenrich et al., 1995; Villante et al., 2001*]. *Mathie et al. [1999a]* suggest that the set of so-called “Samson frequencies” might represent the eigenfrequencies of the most common state of the magnetosphere, with changes in the cavity configuration (size, density etc.) changing the natural frequencies accordingly. At the present time there seems to be evidence for preferred FLR frequencies;

however, their dependence on solar wind and magnetospheric morphology has not yet been determined and requires further study.

In addition to the outer magnetosphere, other regions can act as a cavity for resonant trapping of long-period ULF wave energy. For example, the Alfvén speed gradient at the plasmopause can confine plasmaspheric cavity modes [e.g., *Allan et al., 1986b; Takahashi et al., 2001*]. Indeed, the plasmaspheric and outer magnetospheric cavities are likely to be coupled to each other to some extent, depending on the character of the plasmopause and the wave frequency and wavenumber [e.g., *Allan et al., 1986b; Lee et al., 2002*].

Typically, on the dayside of the magnetosphere the quasi-dipolar closed field line regions of the inner and outer magnetosphere can support closed field line FLRs, the frequency spectrum of the driving fast modes being structured by the natural fast eigenmodes of the global magnetosphere. On the flanks and in the nightside, however, field line stretching can strongly distort the field from its nominal dipolar configuration.

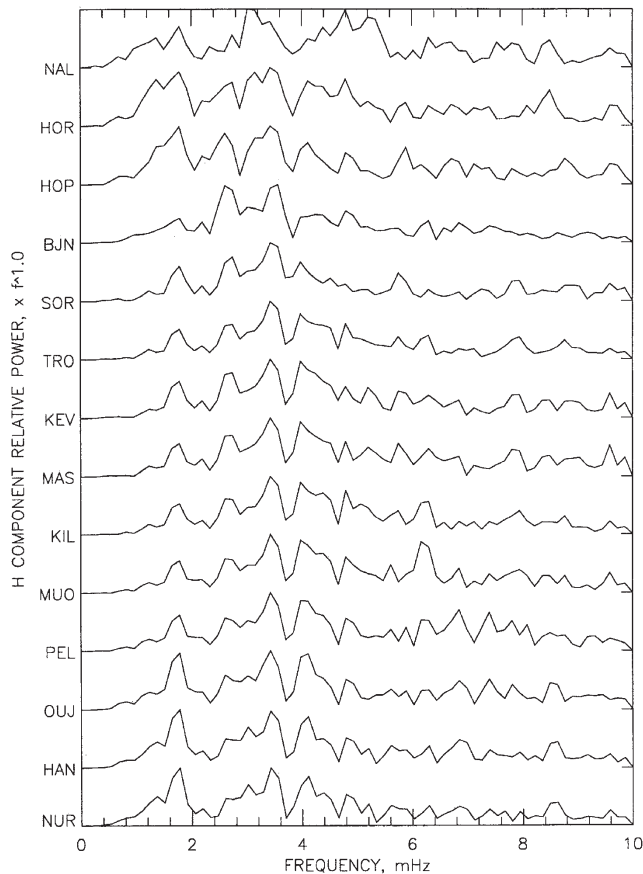


Figure 2. H-component ground-based magnetometer power spectra from selected stations in the IMAGE array from March 8th 1994 between 0610 and 0810 UT. Spectra are stacked in order of decreasing latitude, and the spectra have been whitened by multiplying by frequency (taken from *Mathie and Mann [2000a]*).

This stretching can enable auroral latitude closed field lines to support much lower FLR eigenfrequencies than normal. For realistic plasma densities, these FLR frequencies can be in the mHz range [e.g., *Wanliss et al., 2004*].

3. DAYSIDE/FLANK WAVEGUIDES

The cavity model of FLRs described above has met with considerable success. In this scenario, the magnetosphere is assumed to be a closed axisymmetric cavity which can trap discrete frequency fast mode energy [*Kivelson et al., 1984*] and allow it to excite discrete frequency standing Alfvén waves. However, the fact the fast mode energy generally propagates from the sunward side into the tail led to the proposal that magnetospheric flanks behave more like waveguides [*Samson et al., 1992; Walker, 1992; Wright, 1994*].

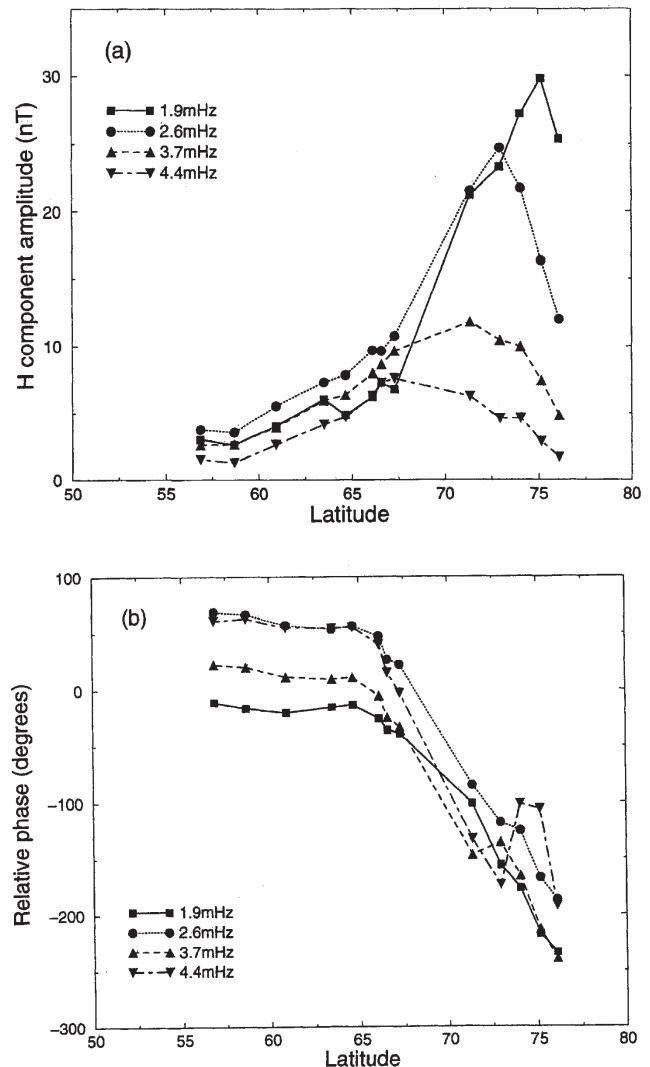


Figure 3. H-component ground-based magnetometer amplitude and phase as function of latitude for 4 discrete wave frequencies from the IMAGE magnetometer array between 1145 and 1345 UT on March 6th 1995. (taken from *Mathie and Mann [2000a]*.)

A simple model of dayside/flank waveguides is shown in Figure 4, which represents a slice in the equatorial plane viewed from above the north pole. The waves indicated represent propagating fast modes that are trapped between an outer reflection point (the magnetopause) and an inner reflection point (or turning point). Clearly, energy entering on the dayside can propagate around the flanks and exit into the tail—unlike in the cavity model. Each flank can be thought of as an independent waveguide, and can be modelled simply as the box model when no periodicity is imposed in y . Such a waveguide is shown for the dusk flank in Figure 5. This should be a reasonable model of

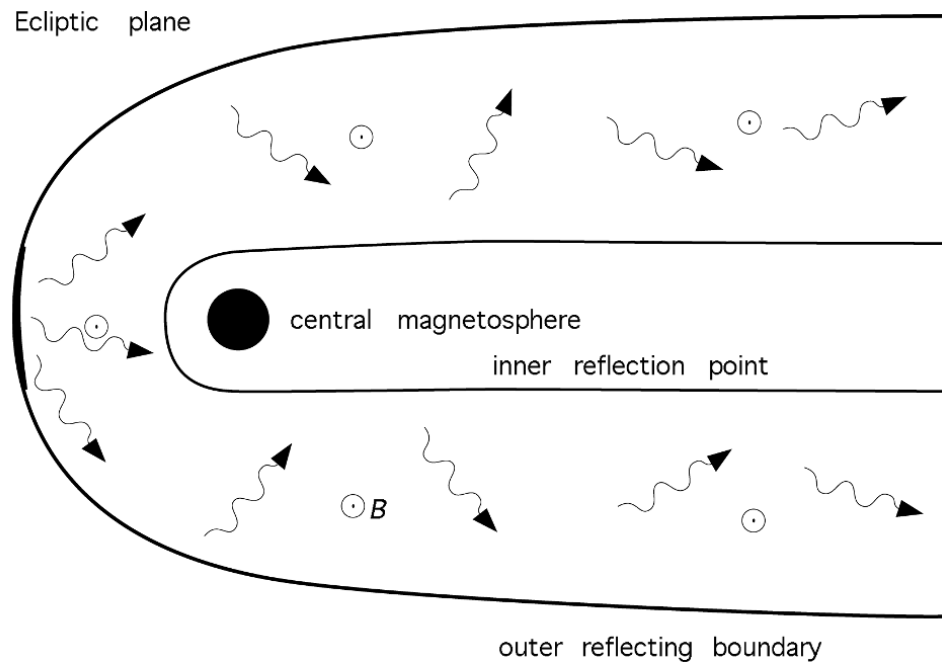


Figure 4. A cross-section of the magnetosphere and magnetotail in the equatorial plane, viewed from above the north pole. The wiggly arrows represent fast mode waves which are trapped between the magnetopause and an inner turning point.

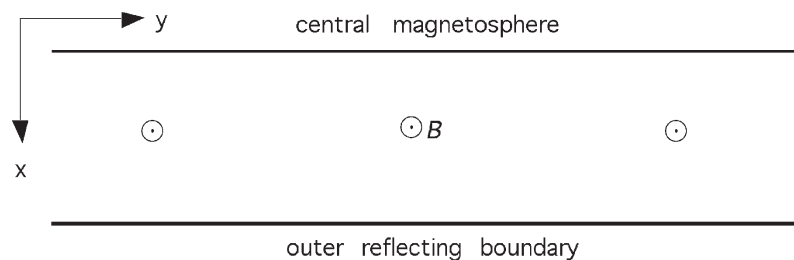


Figure 5. A section of magnetosphere on the dusk flank is modeled as a straight waveguide whose outer boundary is the magnetopause. The radial and azimuthal directions are represented by x and y , respectively.

the flank region, but not the tail (where a different model is adopted).

In the cavity model, it is fast cavity modes that are thought to couple energy into standing Alfvén waves [Kivelson and Southwood, 1985; Allan *et al.*, 1986a; Lee and Lysak, 1989]. In the waveguide model, it is fast waveguide modes which excite Alfvén waves, so it is important to understand how these modes can be excited, how they propagate and disperse along the waveguide, and how they couple to Alfvén waves.

3.1. Waveguide Mode Excitation

The energy source of ULF waves in the magnetosphere can be traced back to the kinetic energy of the solar wind. This

energy must cross the magnetopause before it can exist in the form of a flank waveguide mode on terrestrial field lines. The main processes through which waveguide modes are excited are the same as cavity modes:

- (1) An impulse in solar wind dynamic pressure: Rickard and Wright [1994] showed how a localised push on the magnetopause could excite waveguide modes which couple to Alfvén waves.
- (2) Random buffeting of the magnetopause by fluctuations in the solar wind: Broad-band buffeting of a cavity preferentially excites the natural cavity modes [e.g., Southwood and Kivelson, 1990; Kouznetsov and Lotko, 1995; Wright and Rickard, 1995], and this would also be expected to apply to waveguides.

- (3) The transfer of magnetosheath kinetic energy across the magnetopause by the Kelvin-Helmholtz instability: This was the original mechanism proposed by *Southwood* [1974] and *Chen and Hasegawa* [1974] in the context of the surface mode. Simulations show that this mechanism can also excite waveguide modes too [Mann *et al.*, 1999; Mills *et al.*, 1999].
- (4) Coherent dynamic pressure oscillations in the solar wind have also been suggested as a driver for Pc5 pulsations [Prikryl *et al.*, 1999; Kepko *et al.*, 2002; Stephenson and Walker, 2002], although it is not clear what determines these frequencies. However, even in this case, the accumulation of wave energy in the flank waveguide depends upon the natural frequencies of the waveguide [Mills and Wright, 1999; Walker, 2002].

Once fast modes have been established in the magnetosphere the magnetopause is required to reflect and trap them in the waveguide.

3.2. Magnetopause Boundary Condition

Early models of the magnetopause assumed a perfect reflector [e.g., the cavity models of *Allan et al.*, 1986a; 1986b; *Lee and Lysak*, 1989; and the waveguide model of *Wright*, 1994] and produced results that supported the idea of fast modes being trapped in the magnetosphere. The typical change in density across the dayside magnetopause actually provides a leaky boundary [e.g., *Walker*, 1998; *Mann et al.*, 1999; *Mann and Wright*, 1999; *Freeman*, 2000], but it is now recognised that the jump in flow velocity completely changes the nature of the boundary [Walker, 1998; Mann *et al.*, 1999; Mills *et al.*, 1999].

Figure 6 illustrates the situation for moderate solar wind speeds (upper panel): The slow flow in the vicinity of the sub-solar stagnation point persists over the dayside, and results in a leaky boundary. The flow increases to moderate speeds on the flanks, and the boundary here becomes perfectly reflecting. If the solar wind is faster (lower panel), leaky and perfectly reflecting sections are confined to nearer local noon. The flanks now have a fast flow speed which makes the boundary here over-reflecting. Over-reflection means a fast mode inside the magnetosphere which is incident upon the magnetopause will be reflected with increased amplitude—thus increasing its energy. There is also a transmitted wave in the magnetosheath which is a negative energy wave, and has the effect of removing energy from the sheath flow to balance that supplied to the reflected magnetospheric wave. When the magnetosphere is of finite size, this results in the temporal growth of the magnetospheric fast mode [Mann *et al.*, 1999; Mills *et al.*, 1999]. Indeed, the peak growth rate of the instability can be considered to be the bounded

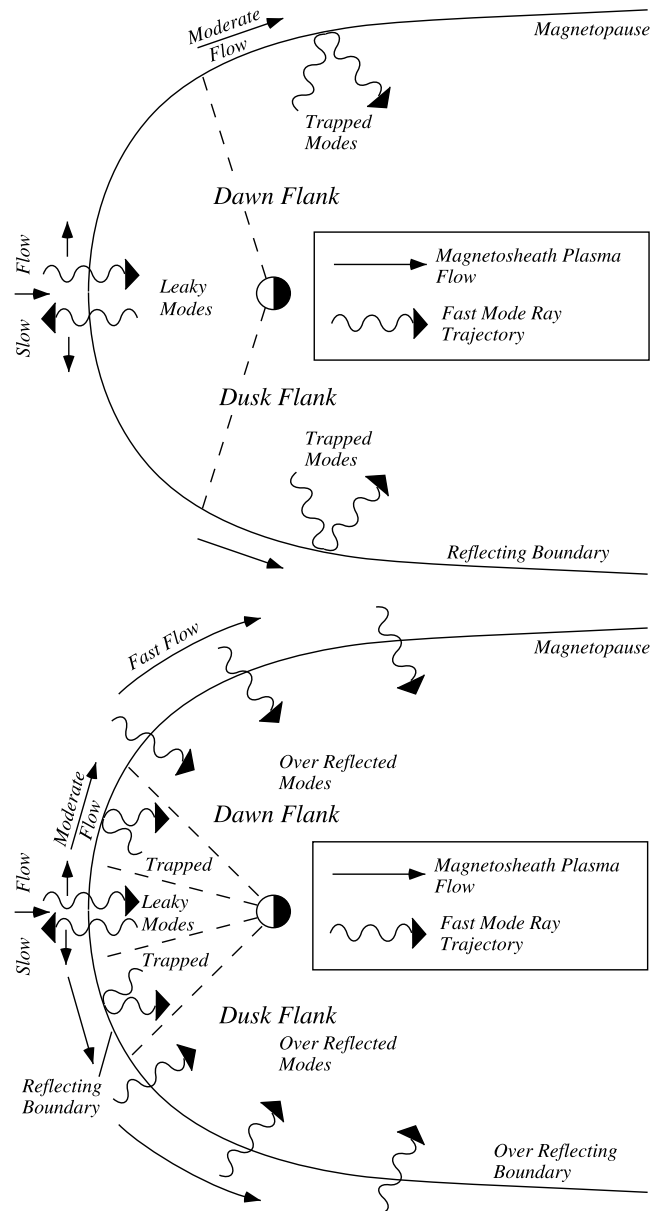


Figure 6. Schematic diagram showing the appropriate waveguide mode magnetopause boundary condition during moderate (top panel), and fast solar wind speeds (bottom panel). Increased magnetosheath flow speed further around the flanks generates regions where the magnetopause changes from leaky to perfectly reflecting. For sufficiently fast magnetosheath flow, the magnetopause boundary may also become Kelvin-Helmholtz shear flow unstable energising growing waveguide modes trapped inside the magnetosphere.

equivalent of the spontaneous emission of sound from a shear flow boundary [see e.g., *Landau and Lifshitz*, 1987; *Mills and Wright*, 1999]. The onset of instability can be described as the point at which stable negative and positive energy

modes coalesce into solutions with complex frequency, one root representing the unstable mode [cf. Cairns, 1979; Mills *et al.*, 1999]. This provides a natural explanation for the well-known preferential flank Pc5 FLR occurrence peak [e.g., Anderson *et al.*, 1990; Cao *et al.*, 1994; Baker *et al.*, 2003].

In a time-dependent scenario the system is better viewed in terms of propagating wave-packets rather than normal modes. In this case it can be argued that the instability is best described through the work done by Maxwell stresses local to the magnetopause boundary rather than by the propagation of a negative energy wave [see e.g., Walker, 2004]. Indeed, in some cases both the transmitted as well as the reflected waves can be amplified [Walker, 2004]. In the case of linear analyses in uniform media, the negative energy wave and Maxwell stress arguments produce the same results [Walker, 2004]. We emphasise that whichever of these complementary descriptions is adopted, our conclusion remains the same: fast waveguide modes can be efficiently energised by the process of over-reflection. The magnetopause shear flow generates growing K.-H. waveguide modes in addition to the usually considered K.-H. unstable surface mode.

Over-reflection hence offers an efficient mechanism for the extraction of energy from the magnetosheath into waveguide modes on the flanks during periods of fast (>500 km/s) solar wind speeds. On the flanks the sheath flow approaches the upstream solar wind speed, and this may explain both the peak in FLR occurrence on the flanks and the strong statistical correlations between enhancements in ground-based Pc5 wave power and solar wind speed [Engebretson *et al.*, 1995; Vennerstrom, 1999; Mathie and Mann, 2001; Mann *et al.*, 2004]. Ground-satellite correlative studies have also found evidence of magnetopause fluctuations, global distributions of discrete frequency fluctuations, and large amplitude FLRs during fast solar wind speeds, supportive of the over-reflection hypothesis [Mann *et al.*, 2002; Rae *et al.*, 2005a].

Figure 7, taken from Rae *et al.*, [2005a] shows the power spectra of global scale signatures of ULF waves in the dusk flank magnetosphere from between 0145 and 0315 UT on 25th November 2001. Panel (a) shows the spectra of dynamic pressure from ACE at the L1 point, and from WIND and GEOTAIL in the near-Earth solar wind (accounting for solar wind propagation to the Earth) whilst panel (b) shows the spectra of total velocity and total magnetic field magnitude from Cluster-3 at the duskside magnetopause. Panel (c) shows approximately azimuthal magnetic field (B_y) and approximately radial electric field (E_x) spectra from Polar at $L \approx 8$, appropriate for the expected polarization of a local FLR. Polar was also on the dusk flank and conjugate to the CANOPUS magnetometer array, the Polar transverse electric and magnetic ULF wave fields each showing the near linear polarisation expected close to the resonant field line [see Rae

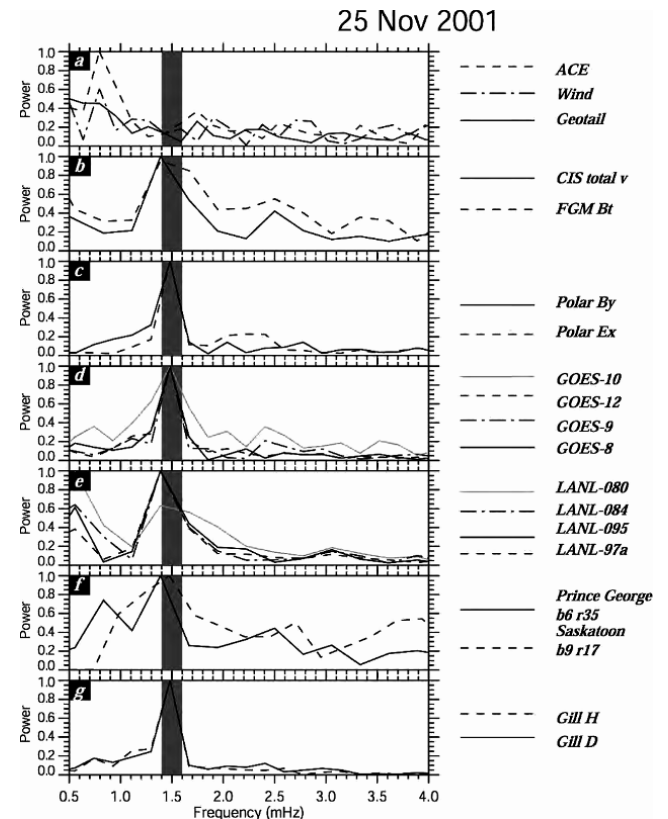


Figure 7. Normalised fast Fourier transform (FFT) power spectra of (a) time-lagged solar wind dynamic pressure, (b) Cluster-3 total magnetic field and total ion velocity (c) Polar Ex and By measurements in field-aligned coordinates, (d) GOES azimuthal magnetic fields, (e) LANL electron energy flux in the 225-315 keV range, (f) SuperDARN line-of-sight velocity data from Prince George and Saskatoon radars, and (g) H- and D-component magnetic fields from the Gillam magnetometer all between 0145-0315 UT on the 25th November 2001. The SuperDARN data are not continuous in this time interval and so the FFT spectra in Figure 7f are between 02-03 UT. The grey shaded area denotes the 1.4-1.6 mHz band. Taken from Rae *et al.* [2005a].

et al., 2005a for more details]. Panels (d) and (e) show the total magnetic field spectra from the GOES fleet, and the spectra of the 225-315 keV electron flux channel from the LANL satellites, at geosynchronous orbit, respectively. Panel (f) shows SuperDARN radar line-of-sight velocity spectra from the Prince George (beam 6, range gate 35) and Saskatoon (beam 9, range gate 17) radars, and finally panel (g) shows the spectra H- and D-component magnetic fields from the Gillam magnetometer. The Cluster observations show repeated magnetopause crossings indicative of magnetopause motion with the same frequency as the FLR characterised on the ground by the CANOPUS magnetometer data, and in situ by Polar, in the same local time sector. The other

magnetospheric data sets also show evidence of the effects of the 1.4-1.6 mHz discrete frequency modes at geosynchronous orbit. The GOES magnetic perturbations show the wave in the same local time sector (GOES 10 and 12), as well as at more distant local times. Finally, the LANL electron flux observations demonstrate the influence of the discrete ULF wave fields on the fluxes of electrons on closed drift trajectories intersecting the FLR. There is no evidence of this discrete frequency in the solar wind dynamic pressure (panel(a)). *Rae et al.* [2005a] concluded the agent linking the common period of the magnetopause motion to the FLR was a K.-H. unstable waveguide mode.

3.3. Absolute and Convective Instabilities

The idea of absolute and convective instabilities applies naturally to waveguides as it describes how a localized initial disturbance propagates along the guide (something that cannot be addressed in a cavity model). As mentioned previously, the energy of the magnetosheath flow has free energy associated with it as does the velocity shear at the magnetopause. The situation for the dusk flank waveguide is shown in Figure 8.

The distinction between an “absolute” and a “convective” instability is illustrated in Figure 9, where a disturbance $f(y, t)$ that is localized in y at $t = 0$ is sketched at subsequent times. The function $f(y, t)$ could represent a localised disturbance on the magnetopause. There will also be some variation of the disturbance in the x and z directions, which takes the form of normal modes. However, the y direction is unique as it is the coordinate along the waveguide, and it is the evolution of perturbations in y that determines the nature of the instability.

In Figure 9a the wavepacket grows exponentially in amplitude with time and does not propagate significantly in the y direction. Thus if we sit at a fixed y (say, y_1) and wait long

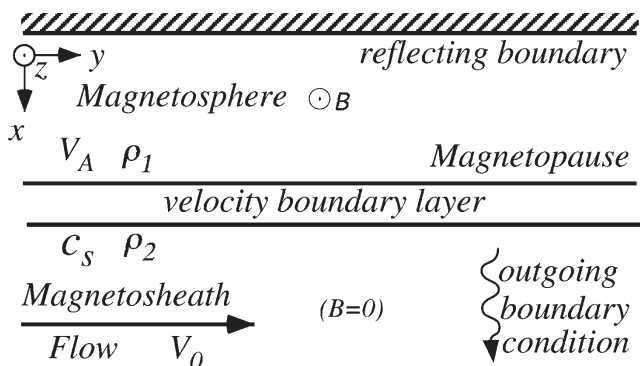


Figure 8. Similar to Figure 5, but a magnetopause boundary layer is introduced across which the equilibrium flow increases to match that in the magnetosheath. Unstable surface and waveguide modes of this system exist subject to an outgoing boundary condition.

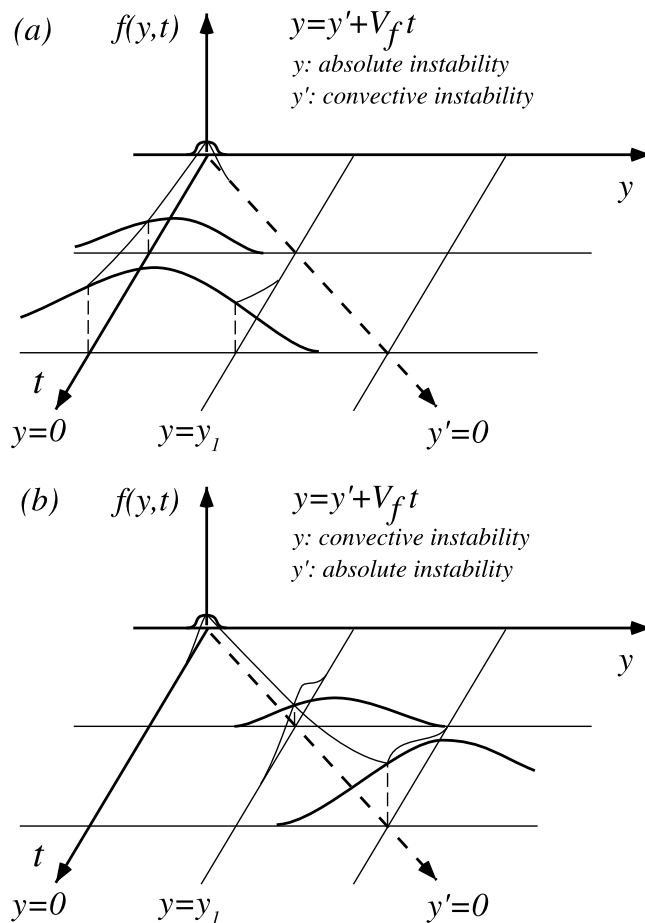


Figure 9. The exponential growth in time of an unstable wavepacket that is localized in y can be classified as “absolutely” or “convective” unstable depending upon its motion in y .

enough we observe a disturbance that grows with time. This is an absolute instability. A similar situation is shown in (b), except that the unstable wavepacket propagates (convects) sufficiently rapidly in the y direction that the signal at $y = y_1$ initially increases, but as $t \rightarrow \infty$ vanishes. This situation is referred to as a convective instability. These definitions depend upon the frame of reference, and transforming to a frame $y' = y - V_f t$, where the frame velocity keeps up with the wavepacket in (b), would mean an observer in the y' frame sees an absolute instability. There is a well-developed theory of this classification [see *Bers*, 1983, and references therein].

To apply these ideas to the magnetospheric flanks, we can think of the y direction as being the azimuthal coordinate. The x direction is the radial coordinate, and a Kelvin-Helmholtz surface mode would have an exponentially decaying structure in x , and some localized wavepacket structure in y . Studies by *Wright et al.* [2000], *Mills et al.* [2000] and *Manuel and Samson* [1993] suggest the surface wave is

convectively unstable in the magnetospheric rest frame and has an e-folding length of an R_E , soon becoming nonlinear causing broadening of the LLBL and saturation.

When discussing the Kelvin-Helmholtz instability, attention invariably focusses on the surface mode. This is probably because it generally has largest growth rate, and dictates the linear behaviour of the system. However, it is often not appreciated that a system like that in Figure 8 has other (waveguide) modes that may be unstable and draw energy from the magnetosheath flow, thus deserving to be termed ‘‘Kelvin-Helmholtz’’ modes. These waveguide modes have an oscillatory variation with x , at least just inside the magnetopause. The stability analysis of these modes by *Wright et al.* [2000] and simulations by *Mills et al.* [2000] shows them to be convectively (rather than absolutely) unstable, with an e-folding length in y of about $20 R_E$. Given the extent of the unstable flank magnetopause is about $30 R_E$, it is likely that these modes will not saturate, and will probably be hard to observe. However, they will be suitable for coupling energy into FLRs [*Wright et al.*, 2002] which are observable.

3.4. Dispersion and Propagation of Waveguide Modes

Once energy has been fed into the fast waveguide modes, much insight into the subsequent behaviour can be gained from ray trajectories. Note that in a waveguide k_y is not quantized (unlike in a cavity), and may take any value. However, the ionospheric boundary conditions quantize the field aligned wavenumber (k_z), and boundary conditions at the magnetopause and inner turning point lead to a dispersion relation between the mode frequency and harmonic number in the radial direction [e.g., *Walker et al.*, 1992; *Wright*, 1994]. For example, for a given k_z and radial mode number we may choose a certain k_y . The dispersion relation will then tell us the mode frequency ω , and the local wavenumber in x . This process can be repeated for all k_y , and a graph of $\omega(k_y)$ plotted, which is known as the dispersion curve for that mode. The phase speed of this mode along the guide is ω/k_y , and it transports energy and information along the guide at the group velocity $\partial\omega/\partial k_y$ —the slope of the dispersion curve.

These ideas can be related to localized disturbances (or wavepackets) by considering a disturbance that is dominated by a particular k_y and k_z . Noting that the dispersion relation determines, the local wavenumber in x can be deduced from

$$k_x^2(x) = \frac{\omega^2}{V_A^2(x)} - k_y^2 - k_z^2 \quad (1)$$

where $V_A(x)$ is the local Alfvén speed. From this equation we see that a radial position (x_t) may exist for which $k_x(x_t) = 0$, and is referred to as the turning point. In the magnetosphere

$V_A(x)$ decreases with radial distance, meaning $k_x^2 > 0$ when $x > x_t$ and $k_x^2 < 0$ when $x < x_t$. Hence the behaviour of the waveguide mode switches from being spatially oscillatory ($x > x_t$) to evanescent/exponential ($x < x_t$). Figure 10 shows a ray trajectory propagating from the magnetopause (x_m) towards the earth ($x = 0$), and being refracted by the increase in Alfvén speed so there is a turning point (x_t). As above, x_t is where $k_x = 0$, so the wave stops travelling towards the Earth and turns around at this point. A little beyond this point (in a Cartesian geometry) the mode can drive an FLR where the waveguide mode frequency matches the local Alfvén frequency, i.e., where

$$\frac{\omega^2}{V_A^2(x_r)} = k_z^2. \quad (2)$$

Comparing (1) and (2) we see that x_r will always lie of the high Alfvén speed side of x_t .

In Figure 10 (lower panel) we show how small k_y wavepackets (trajectory 1) travel down the waveguide slowly (small group velocity), while large k_y (trajectory 3) wavepackets skip along the magnetopause and will propagate at the Alfvén speed just inside this boundary. Intermediate k_y values (trajectory 2) propagate deep enough into the magnetosphere to encounter high Alfvén speeds, but do not have k_y so small that they ‘‘shuffle’’ down the guide. The latter modes will advance down the guide the fastest. *Wright* [1994] demonstrated the equality of the mode group velocity and the bounce-averaged wavepacket speed along the guide.

The above concepts are useful because a general disturbance located around, say, $y = 0$, can be thought of as a superposition of wavepackets whose dispersion and propagation down the guide can be interpreted within this framework. For example, *Wright* [1994] noted that the small k_y modes would be the only ones to linger near $y = 0$. Since the field lines there would have small k_y fast modes which linger on them for several wave periods, these field lines are likely to get FLRs excited on them where the Alfvén frequency of the FLR equals the fast waveguide mode frequency determined through the approximation $\omega(k_y \approx 0)$. Indeed simulations by *Rickard and Wright* [1995] confirmed that these ideas could accurately predict the location and frequency of FLRs excited by an impulsive push on the magnetopause.

Figure 11 shows energy density contours at (a) $t = 20$ and (b) $t = 40$. The push on the magnetopause was confined to $0 < y < 0.2$. Two Alfvén waves (each driven by a different harmonic waveguide mode) are identifiable as the increase in energy density near $x = 0.24$ and $x = 0.56$ which remains in this location. In contrast, the energy density enhancement that moves from $y = 2.5$ (a) to $y = 4.7$ (b) is associated with a wavepacket consisting of a superposition of waveguide modes

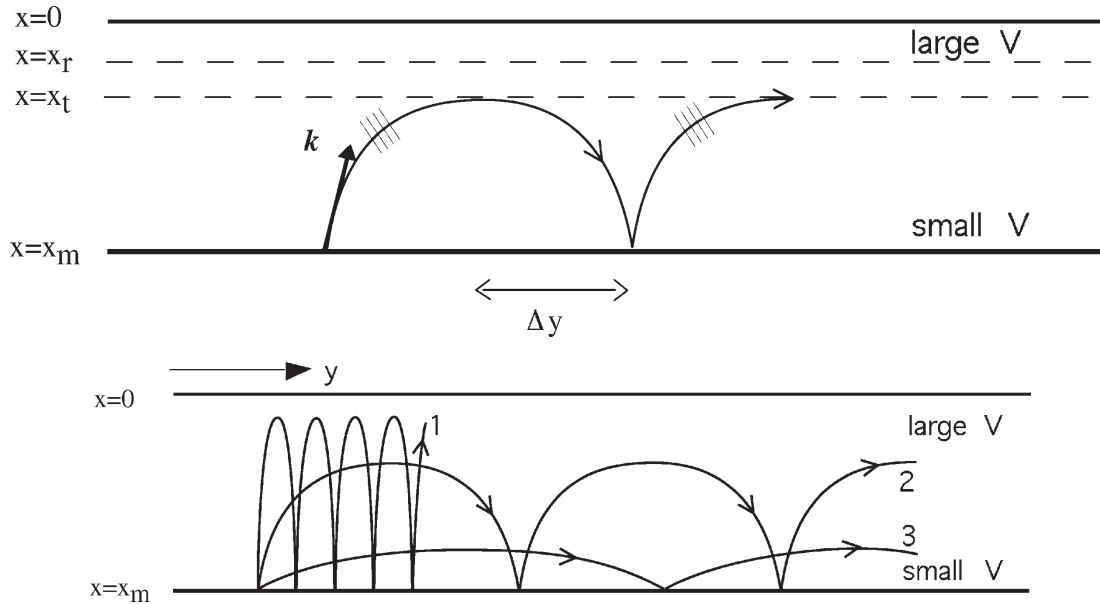


Figure 10. The refraction of a fast mode wavepacket in the flank waveguide (upper panel) may be represented by the indicated ray trajectory, and is associated with a local $k_x(x)$ that vanishes at the “turning point”, x_t . On the high Alfvén speed side of x_t , resonant mode conversion to Alfvén waves can occur (x_r). The lower panel shows three ray trajectories. The average speed with which a ray moves down the guide depends upon the orientation of the wavevector (i.e., the value of k_y), and is equivalent to the group velocity of the corresponding waveguide mode [Wright, 1994].

that are confined to the low Alfvén speed region of the outer magnetosphere. The dispersion of modes along the waveguide means that a clear oscillatory fast mode signature is unlikely to be seen in satellite data. Simulations of such data in a model waveguide by Rickard and Wright [1995] confirmed the absence of a clean fast mode signature (compared to a cavity model, e.g., Lee and Lysak [1989]) but the presence of clear and predictable FLRs. Multiple satellite observations have shown evidence for the downtail propagation of waveguide mode wavepackets down the waveguide [Mann et al., 1997a], although observations such as this are rare.

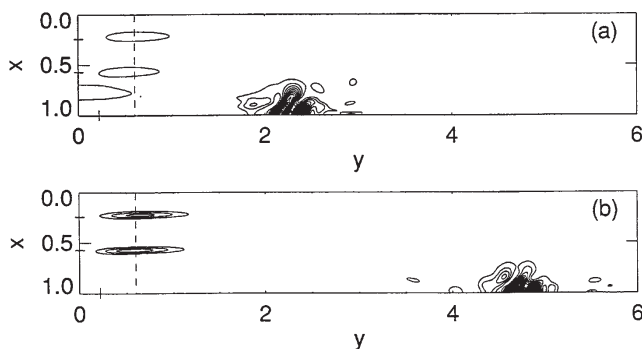


Figure 11. Contour plots of total energy density in a flank waveguide at (a) $t = 20$, and (b) $t = 40$.

A useful diagnostic quantity from observations is the azimuthal phase speed of FLRs, which can be measured by ground-based magnetometer chains or radar. Observations show that two or more FLRs may be driven simultaneously and in certain events they share a common azimuthal phase speed [e.g., Ziesolleck and McDiarmid, 1994; Mathie and Mann, 2000a]. Whether or not this phase speed is common to FLRs may be used to learn something of the nature of how energy enters the magnetospheric waveguide. The simulations of Rickard and Wright [1994, 1995] were driven in a fashion that mimics a solar wind pressure pulse. Similar results were also reported in Wright and Rickard [1995] where the guide was chosen such that two waveguide modes (with different radial harmonic number) would couple to two different FLRs. These results showed that the azimuthal phase speed of the two driven FLRs were different from one another.

When the driving condition was changed so that a pulse ran along the boundary with speed V_b , it was found that the FLRs occurred in the same positions and with the same frequencies as before, but that now the azimuthal phase speeds of the FLRs are identical. These results are summarized in Figure 12 for three different pulse speeds, $V_b = 0.35, 0.7, 1.4$, which are associated with the phase speed shown by dashed lines. The $\omega(k_y = 0)$ frequencies of the FLRs are 1.37 and 2.39, and their k_y values are equal to ω/V_b .

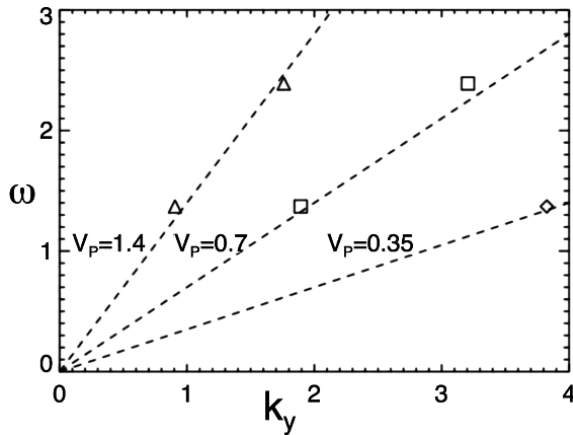


Figure 12. Alfvén pulsation frequency against azimuthal wavenumber for three “running pulse” experiments. $V_b = 0.35$ (diamond), 0.7 (squares), and 1.4 (triangles). In the latter two experiments two pulsations are excited simultaneously. The dashed lines have slopes corresponding to phase speeds matching the pulse speed along the boundary.

The other mechanism thought to operate for exciting waveguide modes is the Kelvin-Helmholtz or over-reflection process [Walker, 1998; Mann *et al.*, 1999], which is likely to occur for high solar wind speeds [exceeding 500 km s^{-1} , Engebretson *et al.*, 1998] on the flanks. Mills and Wright [1999] considered a waveguide bounded by a flowing semi-infinite magnetosheath as shown in Figure 8. For a given radial harmonic, the growth rate depends upon k_y . It is interesting to note that the mode with maximum growth rate has a phase speed (ω/k_y) that corresponds to the over-reflection (spontaneous radiation) condition based upon a local analysis of the magnetopause [McKenzie, 1970; Walker, 1998; Mills and Wright, 1999]. Thus the Kelvin-Helmholtz process will naturally excite waveguide modes with a common phase, and Mills and Wright show that the FLRs these modes drive have the same (i.e., common) phase speed.

The properties of different waveguide energization mechanisms and the associated FLRs have been summarized by Mann and Wright [1999], and show how simultaneous observations of two FLRs can be used to identify the likely mechanism [see also Mathie and Mann, 2000a] if the sheath flow speed and FLR azimuthal phase speeds are known.

3.5. Driven Field Line Resonances

The energy extracted from the solar wind by the excitation of waveguide modes can end up in range of sinks. Some of the energy is lost as the waveguide modes propagate down-tail, however, the low- m waveguide modes with low down-tail group speeds can act as coherent drivers for discrete

frequency FLRs. The energy transfer between the fast compressional waveguide modes and FLRs is uni-directional, Poynting flux being transferred from the waveguide mode into the resonance from both higher and lower L -shells (x in the cartesian box model) [Zhu and Kivelson, 1988]. Once excited, the FLR fields evolve and generate FACs, these FACs ohmically dissipating energy in the resistive ionosphere at the ends of the closed FLR field line [Allan and Knox, 1978; Newton *et al.*, 1979].

Just as for a driven simple harmonic oscillator, the temporal structure of the driven dominantly Alfvénic fields at the resonance are determined by a combination of the directly driven response of the FLR and the oscillation of the FLR fields at their natural frequencies [e.g., Allan and Poulter, 1989; Wright, 1992; Mann *et al.*, 1995]. The waveguide mode response to any solar wind driver, whether it be a solar wind impulse, buffeting, or through magnetopause K.-H. instability, will have a finite lifetime as the mode propagates away down the tail. This time-limited waveguide mode driver dominates the early-time evolution of the FLR; however, as the driver decays at the fixed magnetopause location of the FLR fields, the FLR evolution becomes increasingly dominated by the local natural oscillation of the field-aligned standing Alfvén waves at the resonance. Any longer-lived, multiple, or more continuous excitation of FLR fields can be understood by considering a temporal superposition of the coupled waveguide mode-FLR evolution described below.

Even a single frequency fast waveguide mode will act as a driver with a finite bandwidth if it has finite lifetime. The resulting FLR envelope can be calculated by

$$\Delta L = \left(\frac{d\omega_A(L)}{dL} \right)^{-1} \Delta\omega. \quad (3)$$

where ΔL is the width of the FLR envelope, and $\Delta\omega$ is the driver’s bandwidth. In a box model the envelope width Δx is given by

$$\Delta x = \left(\frac{d\omega_A(x)}{dx} \right)^{-1} \Delta\omega. \quad (4)$$

If the driver is damped, this will also enhance the bandwidth. The smaller the number of wave periods the waveguide mode acts as a coherent driver over, either due to energy loss from FLR excitation or other losses, the broader the bandwidth of the driver. Mann *et al.* [1995] argue using numerical time-domain simulations that the driver bandwidth determined in this way accurately determines the overall width in L of the resonance which is excited. These ideas suggest that only low-amplitude and broad toroidal FLRs will typically be driven in the near-noon magnetosphere where the

magnetopause is expected to be leaky (cf. Figure 6). Flank local times, in the perfectly reflecting or over-reflecting regions, are expected to support higher quality factor waveguide modes which will drive FLRs that have a narrow width in L .

Within the resonance, each excited field line eventually oscillates independently at the local standing Alfvén frequency $\omega_A(x)$. Over time, an initially spatially coherent structure develops spatial structure across L -shells (or x) which narrows with time $\propto t^{-1}$ —a process known as phase mixing [Mann *et al.*, 1995]. For a driven toroidal mode FLR, the effective local wavenumber k_x increases in time, and can be estimated by

$$k_x(x, t) = \frac{d\omega_A(x)}{dx} t. \quad (5)$$

This can be used to define a phase mixing length, the local cross- L spatial scale developed at any time t , [e.g., Mann *et al.*, 1995], as

$$L_{ph} = \frac{2\pi}{k_x(t)} = \frac{2\pi}{\omega'_A(x)t} \quad (6)$$

where $\omega'_A(x) = d\omega_A(x)/dx$ is the local Alfvén frequency gradient. Numerical simulations by Mann *et al.* [1995] demonstrate that the FLR radial (cross- L) scales can be accurately estimated using equation (6). Equation (6) can also be used in numerical simulations to ensure that the fields are being fully resolved by the simulation grid, especially in the critical FLR region. This is important to ensure that energy is not unphysically returned to the fast mode from the FLR due to inadequate resolution of FLR structure [see e.g., the discussion in Mann *et al.*, 1997b].

Of course, phase mixing cannot proceed forever, not least because the energy in the Alfvén waves is ohmically dissipated by the ionosphere. This generates an upper limit to the phase mixing lengths which can be generated by an evolving FLR. Dynamically, ionospheric dissipation limits the FLR spatial scales to $\sim L_I$, where L_I can be determined by the ionospheric damping rate of the Alfvén waves [see Mann *et al.*, 1995, for more details]. This dynamically limited width, L_I , can be considered the time-domain analogy of the finite radial width developed for standing Alfvén eigenmodes through the resolution of the FLR singularity by dissipation due to finite ionospheric conductivity [see e.g., Southwood and Hughes, 1983]. If it is possible, within the FLR lifetime, for L_{ph} to reach kinetic scales (such as a hot ring current ion gyro-radius) which are larger than L_I then kinetic effects will also limit the radial width of the FLR.

The combination of the overall width of the FLR, developed due to the bandwidth of the driver, and the internal structure

developed by phase mixing, typically limited to L_I by ionospheric conductivity, generate the possibility for FLRs to contain internal structure [e.g., Mann, 1997]. Figure 13 shows the temporal evolution of FLR fields resulting from the solution to an initial value problem where the fast cavity/waveguide mode is trapped within the simulation domain. Energy accumulates at the FLR (Figure 13, top) around $x = 0.22$, the overall resonance width narrowing in time as the driver bandwidth narrows as the FLR experiences more cycles of the driver. Eventually all of the fast mode energy coupled to the FLR is deposited there, and the FLR energy envelope stops evolving. Internal to the FLR, the toroidal wave fields (characterised here by azimuthal (y) displacements ξ_y) continue to develop ever decreasing L_{ph} within the resonance envelope

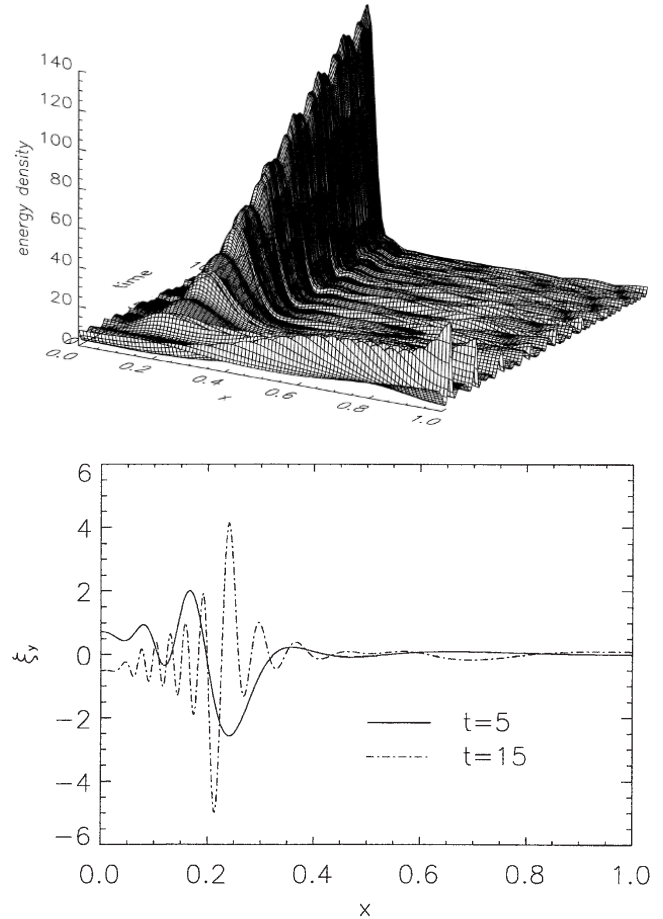


Figure 13. Initial value problem simulation of the development of driven FLR fields in a 1-D magnetosphere bounded by perfectly reflecting magnetopause and inner boundary. Cavity/waveguide mode fields propagate across the box and drive an FLR at $x = 0.22$. Energy accumulates there (top panel), and azimuthal (y) FLR displacement shows the development of $L_{ph} \propto t^{-1}$ (bottom panel). From Mann *et al.* [1995].

(Figure 13, bottom). Indeed, it has been suggested the natural width of an FLR envelope (ΔL) can at times be large enough that adjacent FLRs (driven by different discrete fast modes) will overlap to the extent that spacecraft will observe a continuum of natural Alfvén oscillations, rather than spatially isolated FLRs [McDiarmid *et al.*, 1999].

3.6. FLR Latitudinal Phase

Universal solutions can be derived close to the resonance which demonstrate the relationship between the FLR phase motion and the direction of the local Alfvén frequency gradient [Wright and Allan, 1996]. In the outer magnetosphere, the local standing Alfvén frequency gradient $d\omega_A/dL$ is generally negative and results in poleward phase advance of the FLR fields. However, in the vicinity of the plasma-pause, a steep density gradient can result in $d\omega_A/dL$ becoming positive, and is associated with equatorward phase motion. Such behavior has been observed in radar data [Nielsen and Allan, 1983] and magnetometer data [Dent *et al.*, 2005]. The latter example is rare, probably because of the large separation between magnetometer stations compared to plasma-pause width.

Since the phase mixing Alfvén waves within FLRs generate strong FACs, the internal structure of FLRs can typically contain a number of upward and downward FAC elements. On field lines in the auroral zone, intense upward FAC elements are believed to be related to downward auroral electron acceleration. This cements a link between FLR fields and the potential acceleration (or at least modulation) of auroral electron precipitation on closed field lines in the outer magnetosphere (see section 5), a link which is well-established observationally based on magnetic and optical observations for low- m closed field line FLRs through their poleward phase propagation characteristic [e.g., Samson *et al.*, 1991; 1996; Rae *et al.*, 2005b].

Plate 1 [taken from Rankin *et al.*, 2005] shows the temporal evolution of east-west aligned discrete auroral arcs on 29th October 1998. Arcs periodically reform at the equatorwards edge before propagating polewards across the field-of-view (FOV). The bottom panel shows a keogram constructed from slices through the all-sky-imager FOV, demonstrating the clear polewards phase propagation expected of this ~ 5 mHz FLR. An extensive analysis of this and similar FLR events [e.g., Streltsov and Lotko, 1997; Streltsov *et al.*, 1998; Rankin *et al.*, 1999, 2005] demonstrates a strong argument in favour of a causal connection between discrete auroral arcs and discrete closed-field line FLRs.

Typically, the flank waveguide is excited by sources in the solar wind generating waveguide modes which propagate anti-sunward (cf. section 2.1). However, on stretched field lines at northern auroral latitudes on the flanks one can also

imagine the possibility that tail processes might excite compressional modes in the flank waveguide which propagate sunward rather than anti-sunward. Mathews *et al.* [2004] argue that in this case, the additional Alfvén wave propagation time from the equatorial plane to the ends of these stretched closed field lines can generate FLRs whose phase is reversed into an equatorward propagation. Plate 2 [from Mathews *et al.*, 2004] shows meridian scanning photometer observations of equatorward propagating discrete arcs on the dusk flank. Using magnetic and optical observations of these sunwards propagating discrete arcs, Mathews *et al.* [2004] demonstrate how field line stretching can generate the observed equatorward arc propagation away from the poleward edge of the auroral oval consistent with Plate 2.

4. WAVES IN THE MAGNETOTAIL WAVEGUIDE

Satellite observations of MHD waves in the magnetotail indicate the presence of fast waveguide modes [e.g., Elphinstone *et al.*, 1995] and Alfvén waves on both the lobe and plasma sheet boundary layer (PSBL) field lines [e.g., Wygant *et al.*, 2000; Keiling *et al.*, 2005]. When these field lines are mapped to the ground it is thought that the waves can modulate electron precipitation and auroral emissions [e.g., Samson *et al.*, 1991; Wright *et al.*, 1999], since current densities can be a few μAm^{-2} in the ionosphere. Indeed, Lyons *et al.* [2002] suggest the auroral poleward boundary intensifications are a produced by large-scale ULF oscillations in the magnetotail. Some of these studies indicate that the waves are associated with a global reconfiguration of the tail as evidenced by the presence of bursty flows and substorm activity. These may serve to release energy into the waveguide modes.

4.1. Equilibrium Tail Waveguide

Figure 14 shows a simple model of the tail waveguide. A dense warm plasma sheet is bounded by open low-density lobe field lines. The transition between the two occurs over the PSBL where a strong variation in Alfvén speed exists. Beyond the tail lobes lies the fast flowing magnetosheath. Note that this velocity shear is stable for fast waveguide modes owing to the orientation of the equilibrium magnetic field. Indeed, the modes may even be slightly leaky [Mills and Wright, 2000].

Although the PSBL field lines are closed, they may be so distended that they are effectively open on the timescale of waves seen in the tail. Wave coupling in an equilibrium like that in Figure 14 has been studied by Liu *et al.* [1995]. They showed how coupling between the fast mode and an Alfvén resonance was possible in much the same way as in the cavity mode model. We note that they restricted their analysis to

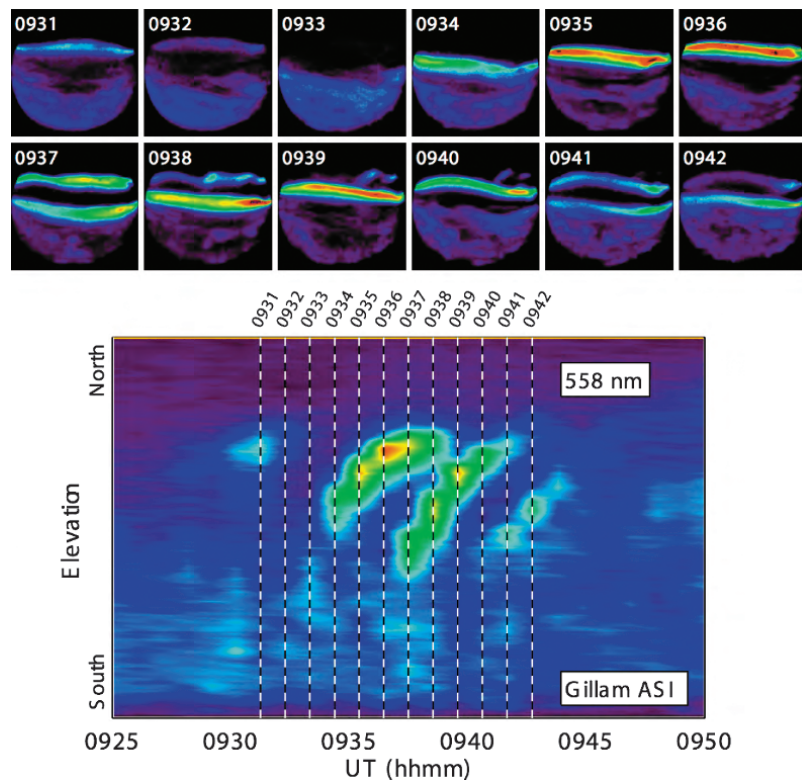


Plate 1. Series of 558 nm images from 29th October 1998 from the all-sky-imager (ASI) data from Gillam, Manitoba (top two rows), from the NORSTAR optical array (part of the Canadian Auroral Network for the OPEN Program Unified Study (CANOPUS) array [Rostoker *et al.*, 1995] which now operates as the Canadian Geospace Monitoring Program). Keogram constructed from the ASI data (bottom panel) showing the periodic poleward motion of the arcs consistent with that expected from a FLR. From Rankin *et al.* [2005].

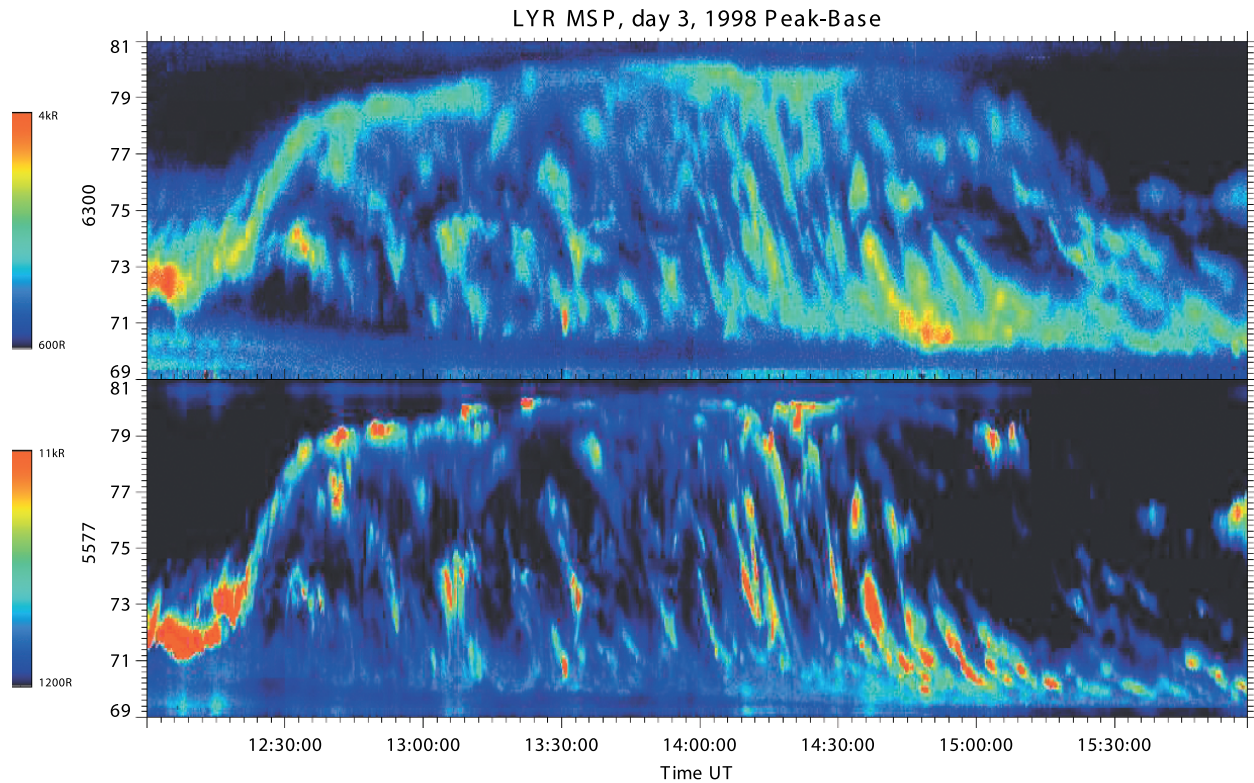


Plate 2. Longyerbyen Meridian Scanning Photometer date from 3rd January 1998. Auroral emissions in the 630 nm (top panel) and 557.7 nm (bottom) panel wavelengths. Following substorm-related polewards expansion around 1230 UT (MLT \approx UT + 2.5 hours), periodic discrete arcs especially between 14-15 UT (shown to be east-west aligned in all-sky-camera data) are seen to periodically propagate equatorwards from the polewards cutoff in the 630 nm emissions (believed to be a proxy for the open-closed field line boundary). From *Mathews et al.* [2004].

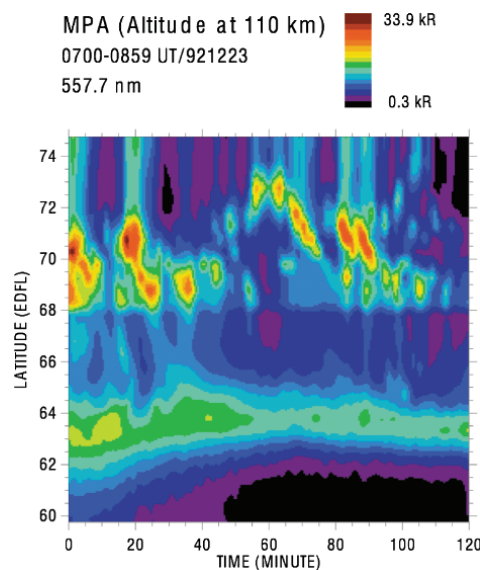


Plate 3. Meridian scanning photometer data from Gillam and Rankin Inlets from 23rd December 1992 as a function of UT at 558 nm. The lower station ($<68^\circ$) has intermittent cloud cover.

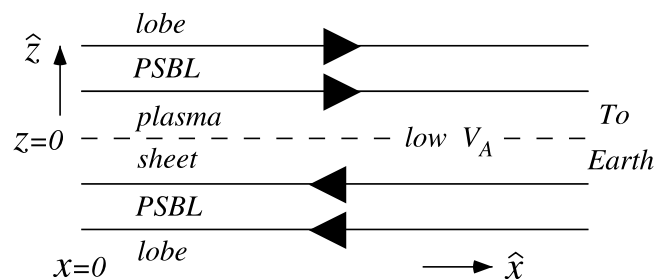


Figure 14. A simple model of the magnetotail waveguide. The dense plasma sheet has a low V_A which increases through the PSBL to the high V_A lobe.

a single value of the field-aligned wavenumber k_{\parallel} , meaning a study of how the waves propagate along the tail was not possible.

4.2. Propagation Along the Tail

Wright *et al.* [1999] considered the two dimensional temporal behaviour of waves in an equilibrium like that in Figure 14 (i.e., quantities depend upon x , z and t). In terms of normal modes or ray trajectories we need to consider a continuum of k_{\parallel} values unlike those on closed field lines. For a given cross-tail wave number k_{\perp} and harmonic mode number in the z direction, they showed how the fast mode dispersion relation gives $\omega(k_{\parallel})$, as sketched in Figure 15(a) and represented by the curved line. The slope of this curve gives $V_{g\parallel}(k_{\parallel})$ —the speed with which this mode (wavepacket) travels along the waveguide. The phase speed of this mode is ω/k_{\parallel} , and on a certain field line (z) this may equal the local Alfvén speed ($V_A(z) = \omega/k_{\parallel}$) where coupling of fast mode energy to the Alfvén wave can occur. This condition may be identified by considering the straight line in Figure 15(a), which has a slope of $V_A(z)$: The intersection of this line with the fast mode dispersion relation defines $\omega_A(z)$ and $k_{\parallel A}(z)$, which are the frequency and parallel wave number of the Alfvén wave excited on the field line at the chosen z . Evidently, a different field line with a different Alfvén speed, will have an Alfvén wave excited on it with different values of ω_A and $k_{\parallel A}$ determined by altering the slope of the straight line in Figure 15(a) appropriately, and finding the intersection.

The properties described above are illustrated (for the northern half of the tail) in Figure 16 where some localized source of waves (perhaps a substorm) initially existed. Some time later the fast mode component k_{\parallel} (which has frequency $\omega(k_{\parallel})$) has travelled down the guide with speed $V_{g\parallel}(k_{\parallel})$ and excited an Alfvén wave of frequency ω_A and wave number $k_{\parallel A}$ on a field line where $\omega_A(z) = k_{\parallel} V_A(z) = \omega$ and $k_{\parallel A} = k_{\parallel}$. Thus the phase speed of the fast mode k_{\parallel} component and the Alfvén wave it excites are the same. The Alfvén wave

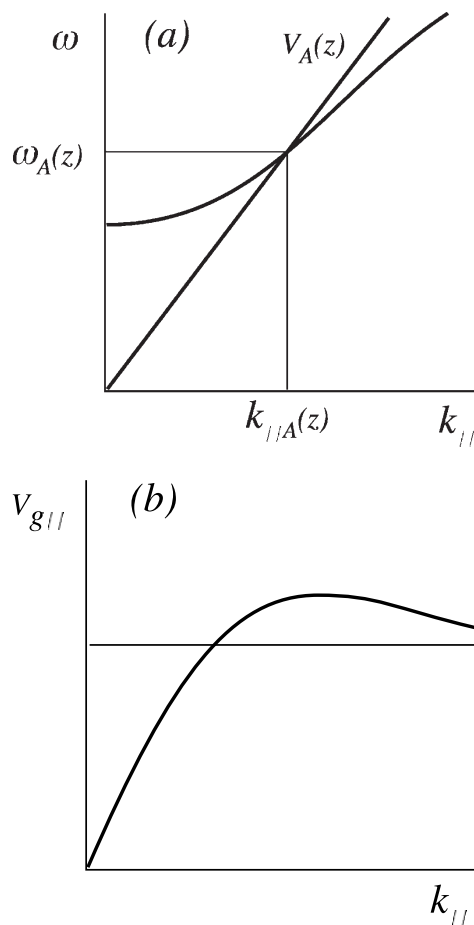


Figure 15. (a) The dispersion relation for a fast waveguide mode (of given k_{\perp}) is shown, as the curved line, along with that for Alfvén waves on a particular field line. The point of intersection identifies the frequency and parallel wavenumber of Alfvén waves that will be excited on that field line (straight line). (b) The group velocity of the fast waveguide modes is found from the slope of the dispersion diagram in (a).

propagates with speed $V_A(z)$, and so runs ahead of the fast mode since $V_A(z)$ is generally greater than $V_{g\parallel}$ of the mode coupling to it.

In terms of ray trajectories, the fast mode is refracted by the change in Alfvén speed and has a turning point (z_t) which confines it to the center of the tail. This is shown as the striped region in Figure 16, lower panel, for a given k_{\parallel} component. However, since a waveguide supports a continuum of k_{\parallel} values, we can repeat the above analysis for a range of k_{\parallel} . The result is that Alfvén waves are excited in the lobe and PSBL with frequencies ($\omega_A(z)$) and wavenumbers $k_{\parallel A}(z)$ as described above. Indeed simulations of this system [Allan and Wright, 1998; 2000] are neatly interpreted using this theory, as are observations [Wright *et al.*, 1999].

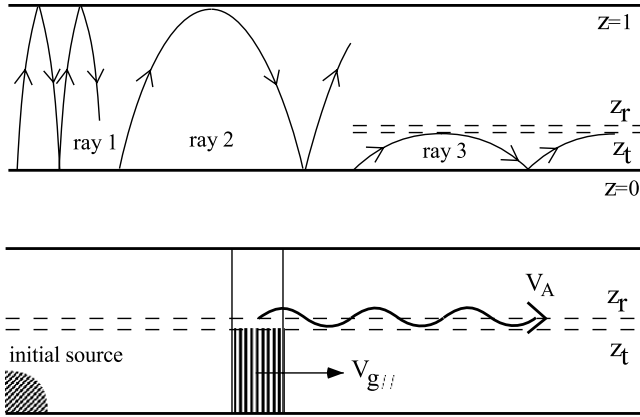


Figure 16. Ray trajectories of fast modes from the centre of the plasma sheet ($z = 0$) towards the magnetopause ($z = 1$) for different wavenumbers is shown in the upper panel (only the northern half of the magnetotail waveguide is shown). The lower panel considers an initial, localized source of fast mode energy to be a superposition of waveguide modes having a range k_{\parallel} values. One particular k_{\parallel} component is shown propagating along the guide with speed $V_{g\parallel}$, and coupling to an Alfvén wave.

Figure 17 show results of simulations taken from *Allan and Wright* [2000] for a small value of k_y that allows us to decompose the waves' energy density into (approximately) E_F and E_A associated with the fast and Alfvén modes. The top panel is a contour plot of E_F , and the lower panel is of E_A . Only the

northern half of the tail is shown. There is a uniform lobe region $0.2 < z < 0.8$, and the PSBL main Alfvén variations is between $0.1 < z < 0.2$. The initial wave energy was injected as a fast mode through the $z = 0$ boundary over $0 < x < 0.48$. Figure 17 shows the state at a much later time following wave coupling.

In Figure 17 note that E_F is concentrated in plasma sheet (see ray 3 in Figure 16) and travels along the guide more slowly than the Alfvén waves which run ahead - particularly in the high Alfvén speed lobe.

In the tail waveguide there are no special “resonant field lines”, but rather a layer of PSBL and lobe field lines on which Alfvén waves are excited, as is evident in the lower panel of Figure 17. On a given field line (z) the location of the Alfvénic disturbance that is excited is predicted in terms of distances travelled from the source based upon the speeds $V_{g\parallel}(k_{\parallel})$ and $V_A(z)$. The phase of the Alfvén waves will depend upon (x, z) and t . If the source is at $x = z = t = 0$, the simulations show the phase is simply given by

$$\phi = k_{\parallel A}(z)x - \omega_A(z)t \quad (7)$$

to an excellent approximation. This accounts for the almost plane Alfvén wave seen in the lobe ($x > 3$) and strong phase mixing of Alfvén waves in the PSBL ($0.1 < z < 0.2$).

The phase structure in the above equation evidently corresponds to propagation in x (i.e., earthward). *Allan and Wright* [2000] note that the large propagation speeds in the tail means a near-earth satellite will almost certainly see not only

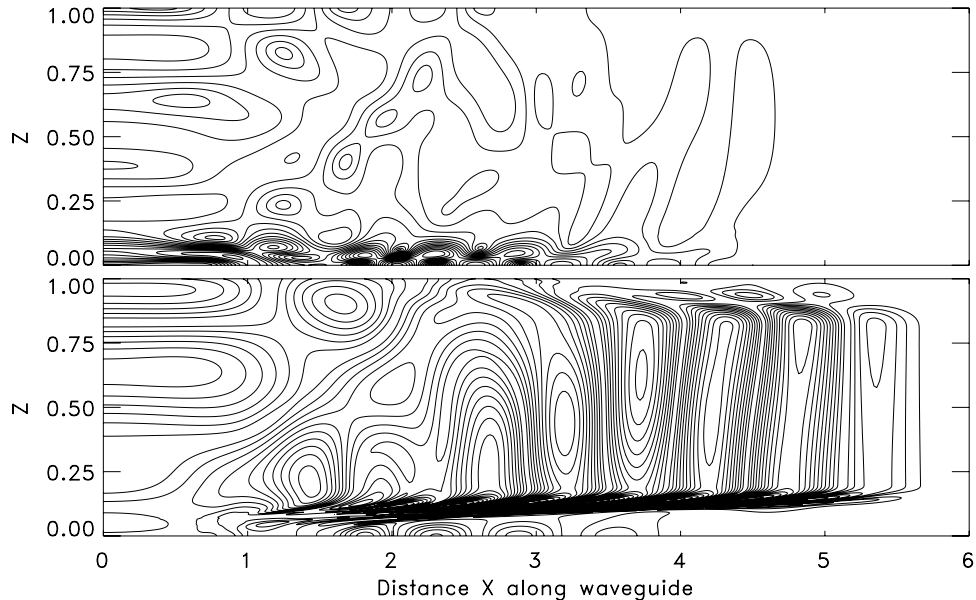


Figure 17. Contour plots of a snapshot of fast (upper panel) and Alfvén (lower panel) energy densities for the northern half of the magnetotail following the earlier injection of fast mode energy in the vicinity of $(0, 0)$.

the earthward propagating wave, but also a wave reflected from the ionosphere. If there is efficient reflection of the incident wave, the superposition would be observed to have a local standing structure. However, if ionospheric reflection is poor, predominantly earthward propagation will be observed. This raises the possibility of PSBL and lobe waves being used to understand details of Alfvén wave energy loss, such as due to Pedersen currents and electron energization (see Section 5).

Recent observations by *Keiling et al.* [2005] [furthering those reported by *Wygant et al.*, 2000, 2002 and *Keiling et al.*, 2001] show that near-earth spacecraft throughout most of the tail lobe see good reflection of the incident Alfvén wave, resulting in a standing wave with a net Poynting flux close to zero. These waves have a large perpendicular scale, and evidently suffer little energy loss between the spacecraft and the earth. As the poleward edge of the PSBL is approached, spacecraft see just earthward propagating Alfvén waves, indicating substantial energy loss to the ionosphere. A significant component of this energy loss may occur as a result of energy conversion into field-aligned motion of auroral electrons [see Section 5 and *Wygant et al.*, 2002; *Wright et al.*, 2003].

The character of Alfvén waves in the PSBL itself is intriguing: They are generally of much larger amplitude than those in the lobe and have much smaller (“phasemixed”) perpendicular scales, as well as exhibiting a variety of propagation characteristics. Long period waves (40-300 s) can be classified as either earthward propagating (most commonly) or standing (occasionally), with most Poynting flux directed earthward and indicating energy loss earthward of the spacecraft. In the period range 40-67 s clear examples of well-phasemixed standing waves were found. Waves with periods between 6-24 s showed independent wave packets propagating both earthward and tailward. These waves, and those reported by *Elphinstone et al.* [1995] and *Wright et al.* [1999] all followed substorm onset.

4.3. Latitudinal Structure

Tracing the lobe and PSBL field lines to the ionosphere maps the z coordinate on to the latitudinal coordinate, and allows us to study the latitudinal structure of ionospheric signatures. For example, *Wright et al.* [1999] show how the phase speed in z and the local phase mixing length in z are both inversely proportional to dV_A/dz . This means that in the PSBL (where dV_A/dz is large) strong phase mixing will produce small scales in z and lead to large field-aligned currents here, which may produce optical auroral displays. The phase velocity of these features will be equatorward, according to this theory.

These features are evident in the meridian scanning photometer data in Plate 3, which is taken from *Wright et al.*

[1999]: The enhanced emissions centered on 70°N have local times 0100 – 0300 hours and map to the PSBL. Note that the emissions at higher latitudes take the form of a fainter tail attached to the PSBL emissions, but have a much larger latitudinal phase velocity and lower intensity than those associated with the PSBL. This can be understood from the theory, since the higher latitude emission tail will be on lobe field lines where dV_A/dz is smaller. This will result in a larger local phase mixing length, weaker FACs, less auroral brightening, and a much larger latitudinal phase speed. The degree of phase mixing depends upon when and where the waves are observed. *Wright et al.* [1999] show the phase velocities and period of auroral brightenings are in good agreement with a wave source $35 R_E$ downtail. These type of auroral enhancements are very similar to those reported by *Lyons et al.* [2002] who placed them on field lines poleward of the plasma sheet, and found they were correlated with bursty flows in the tail.

5. ALFVÉN WAVE ENERGY BUDGET

Alfvén waves, whether on dayside or nightside field lines, have a current circuit associated with them. When the current flows through the ionosphere, in the form of a Pedersen current, there will be Ohmic dissipation. Indeed, this is generally thought to be the principal mechanism through which the waves are damped [*Allan and Knox*, 1979; *Newton et al.*, 1979].

As the ionosphere is approached the converging magnetic field geometry intensifies the field-aligned current density (j_{\parallel}) to several μAm^{-2} . These currents are carried mainly by electrons streaming along the field lines ($v_{e\parallel}$), and a large j_{\parallel} requires a large $v_{e\parallel}$. Indeed, it is the energy of these electrons that is responsible for producing the optical aurora. The necessity of electron acceleration is beginning to identify common physics in the traditionally separate areas of auroral acceleration and ULF waves.

5.1. Electron Dynamics

Early studies of ULF waves employed single-fluid MHD (in which the electron mass is neglected). Recognition of the importance of electron dynamics has led to a number of studies recently in which the two-fluid approximation has been employed [e.g., *Streltsov and Lotko*, 1997; *Rankin et al.*, this issue, and references therein; *Wright et al.*, 2002], and enables processes such as electron energization to be investigated.

Rönmark [1999] and *Wright et al.* [2002] show how the converging field geometry leads to an acceleration region of roughly $1 R_E$ extent lying above the F-region on upward current (downgoing electron) field lines. The electrons will have

energies of a few keV, meaning that they cross the accelerator region in ~ 1 s, which is much less than the period of a Pc5 wave. Thus the fields are approximately steady, and much of the steady-state auroral acceleration literature may be of interest [Wright, 2005, and references therein].

Quasi-steady auroral electron acceleration has received much attention for both upgoing and downgoing electron sections of the current circuit [e.g., Knight, 1975; Rankin *et al.*, 1999; Vedin and Rönmark, 2005; Boström, 2003; Cran-McGreehin and Wright, 2005] using the Vlasov equation. Other studies have employed particle-in-cell and hybrid schemes [Damiano and Wright, 2005; Watt *et al.*, 2004].

5.2. Observations

Recent observations have shown that our view of a ULF wave depends upon how we choose to observe it. For example, Scofield *et al.* [2005] show how the latitudinal scale in radar data can be several 100 km, while in FAST data the same event has structure at 50 km. The latter scale is roughly $10\lambda_e$, where λ_e is the electron inertial length ($\lambda_e^2 = m_e/\mu_0 n e^2$) and is 5 km for $n = 1 \text{ cm}^3$ (n is the magnetospheric number density). If the perpendicular scale of the wave is several λ_e , we can expect that electron mass will start to become important.

Chaston *et al.* [2002] showed that the energy flux density carried by electrons at FAST can be similar to the Poynting vector. Vaivads *et al.* [2003] found the downgoing Poynting vector at Cluster (when mapped to the ionosphere) was the same as the electron energy flux density recorded by DMSP. These studies suggest that a significant amount of Alfvén wave energy can be expended in accelerating electrons compared to the traditional Joule heating mechanism.

5.3. Alfvén Wave Damping

Wright *et al.* [2003] showed that if the latitudinal scale in the ionosphere (λ) is equal to λ_e , then there is equipartition between magnetic and electron kinetic energy densities. Observations suggest $\lambda/\lambda_e \sim 5\text{-}100$, meaning that little energy resides in the electrons. However, the electrons travel at high speeds at the B/n peak, and so the kinetic energy flux density can be significant. Wright *et al.* [2003] calculated the ratio of electron energy flux density to the Poynting vector. In terms of the length scale λ_0 , where

$$\lambda_0^3 = \frac{b \sum_p m_e}{2\mu_0 n^2 e^3} \quad (8)$$

Joule dissipation dominates when $\lambda > \lambda_0$, and electron energization dominates when $\lambda < \lambda_0$. (\sum_p is the height integrated Pedersen conductivity, and b is the azimuthal magnetic field perturbation above the ionosphere.)

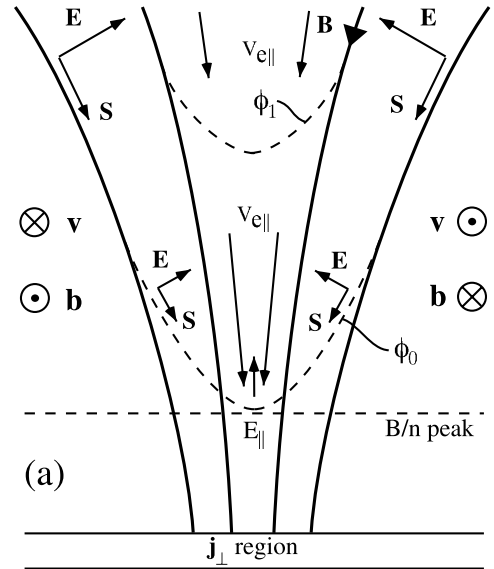


Figure 18. A schematic of an upward FAC in a meridional lane. The converging field geometry produces large j_{\parallel} and downgoing electron speeds as the ionosphere is approached.

Evidently as λ decreases, current densities increase and $v_{e\parallel}$ increases. For a typical fully phased mixed FLR ($\lambda \sim 25$ km at the ionosphere) electrons represent a sink of energy for the Alfvén wave that exceeds Joule heating by a factor of 3. Figure 18 shows how the Poynting vector lies along contours of electric potential (in a quasi-steady Alfvén wave carrying an upward current). The contours are U-shaped, which is familiar from auroral acceleration work. The Poynting vector directs energy into the region where electrons are accelerated, from which it emerges as electron kinetic energy. In the downward current region cold ionospheric electrons will be accelerated upward, and will drain energy from the Alfvén wave at a similar rate to that of the downgoing electrons in Figure 18.

6. SUMMARY

In this review we have examined how ULF wave eigenmodes of the outer magnetosphere can be used to understand a wide range of solar-terrestrial coupling phenomena. The concepts of waveguide modes driving FLRs have been remarkably successful in explaining the observed properties of ULF modes both on closed field lines on the dayside and flanks of the magnetosphere, as well as in the magnetotail on effectively open field lines mapping to the poleward edge of the nightside auroral oval.

There is increasing evidence that the energy transported by ULF waves within the magnetosphere is dynamically

important for a range of processes. In this review we have demonstrated the important role played by ULF waves in transporting solar wind energy into the dayside magnetosphere, and coupling energy initially stored in the magnetotail from the tail into nightside auroral emissions. These ULF processes provide a pathway for the deposition of energy in the ionosphere either by ohmic dissipation or through the acceleration of auroral electrons and excitation of optical auroral arcs. *Greenwald and Walker* [1980] argue that ULF FLR ohmic energy dissipation in the ionosphere is at least as important as that dissipated during a small substorm per unit area per unit time. Similarly, recent studies of Earthward-directed Alfvén wave Poynting flux in the PSBL in association with auroral arcs [e.g., *Wygant et al.*, 2000; *Keiling et al.*, 2002] have demonstrated that ULF wave energy transport is likely one of the dominant processes for magnetosphere-ionosphere energy transport in the magnetotail. Indeed a dynamic view of the substorm current wedge is in terms of FACs carried by ULF Alfvén waves propagating between the reconnection site and the ionosphere. Given the sometimes large amplitudes of Pc5 ULF wave electric fields in the equatorial plane, ULF waves have also been suggested as a component of the elusive MeV electron acceleration process [e.g., *Rostoker et al.*, 1998; *Mathie and Mann*, 2000b; *Elkington et al.*, 2003; *Mann et al.*, 2004] which energises the outer radiation belt (see e.g., *Friedel et al.* [2002] or *O'Brien et al.* [2003] for reviews of radiation belt dynamics).

The magnetospheric waveguide paradigm has met with remarkable success in explaining the ULF eigenmode structure in the outer magnetosphere. While some questions remain, notably further examination of the mechanisms by which these cavity/waveguide modes are excited, the paradigm offers a solid basis for future investigations of the dynamical effects of ULF wave fields on magnetospheric processes including energy transport and energetic particle-ULF wave interactions in the auroral zone and Van Allen belts.

Acknowledgments. The authors would like to thank W. Allan, P. Damiano, Z. Dent, R. Elphinstone, A. Hood, A. Longbottom, J. Mathews, R. Mathie, F. Menk, D. Milling, K. Mills, L. Ozeke, I.J. Rae, and M. Ruderman for fruitful collaborations and discussions. IRM is supported by a Discovery Grant from Canadian NSERC.

REFERENCES

- Allan, W., and F.B. Knox, A dipole field model for axisymmetric Alfvén waves with finite ionosphere conductivities, *Planet. Space Sci.*, 27, 79, 1979.
- Allan, W., S.P. White, and E.M. Poulter, Impulse-excited hydromagnetic cavity and field-line resonances in the magnetosphere, *Planet. Space Sci.*, 34, 371, 1986a.
- Allan, W., E.M. Poulter, and S.P. White, Hydromagnetic wave coupling in the magnetosphere - Plasmopause effects on impulse excited resonances, *Planet. Space Sci.*, 34, 1189, 1986b.
- Allan, W., and E.M. Poulter, Damping of magnetospheric cavity mode: A discussion, *J. Geophys. Res.*, 94, 11,483, 1989.
- Allan, W., and A.N. Wright, Hydromagnetic wave propagation and coupling in a magnetotail waveguide, *J. Geophys. Res.*, 103, 2359, 1998.
- Allan, W., and A.N. Wright, Magnetotail waveguide: Fast and Alfvén waves in the plasma sheet boundary layer and lobe, *J. Geophys. Res.*, 105, 317, 2000.
- Anderson, B.J., M.J. Engebretson, S.P. Rounds, L.J. Zanetti, and T.A. Potemra, A statistical study of pulsations observed by the AMPTE/CCE magnetic fields experiment, 1, Occurrence distributions, *J. Geophys. Res.*, 95, 10,495, 1990.
- Baker, G.J., E.F. Donovan, and B.J. Jackel, A comprehensive survey of auroral latitude Pc5 pulsation characteristics, *J. Geophys. Res.*, 108, doi:10.1029/2002JA009801, 2003.
- Bers, A., Space-time evolution of plasma instabilities - absolute and convective, in *Handbook of Plasma Physics*, edited by M.N. Rosenbluth and R.Z. Sagdeev, Volume 1: Basic Plasma Physics I, edited by A.A. Galeev and R.N. Sudan, North-Holland Publishing Company, 1983.
- Boström, R., Kinetic and space charge control of current flow and voltage drops along magnetic flux tubes: Kinetic effects, *J. Geophys. Res.*, 108, 8004, doi:10.1029/2002JA009295, 2003.
- Cairns, R.A., The role of negative energy waves in some instabilities of parallel flows, *J. Fluid Mech.*, 92, 1, 1979.
- Cao, M., R.L. McPherron, C.T. Russell, Statistical study of ULF wave occurrence in the dayside magnetosphere, *J. Geophys. Res.*, 99, 8731, 1994.
- Chaston, C.C., J.W. Bonnell, L.M. Peticolas, C.W. Carlson, and J.P. McFadden, Driven Alfvén waves and electron acceleration, *Geophys. Res. Lett.*, 29 (11), doi:10.1029/2001GL013842, 2002.
- Chen, L., and A. Hasegawa, A theory of long-period magnetic pulsations, 2, Impulse excitation of surface eigenmode, *J. Geophys. Res.*, 79, 1033, 1974.
- Cran-McGreehin, A.P., and A.N. Wright, Current-voltage relationship in the downward field-aligned current region, *J. Geophys. Res.*, 110, doi:10.1029/2004JA010870, 2005.
- Cummings, W.D., R.J. O'Sullivan, and P.J. Coleman, Standing Alfvén waves in the magnetosphere, *J. Geophys. Res.*, 74, 778, 1969.
- Damiano, P.A., and A.N. Wright, 2D hybrid MHD-kinetic electron simulations of an Alfvén wave pulse, *J. Geophys. Res.*, 110, A01201, doi:10.1029JA010603, 2005.
- Dent, Z.C., I.R. Mann, J. Goldstein, F.W. Menk, and L.G. Ozeke, Coordinated IMAGE satellite and ground-magnetometer observations of a cross-phase reversal at a steep plasmopause, *J. Geophys. Res.*, To be Submitted, 2005.
- Dungey, J.W., Electrodynamics of the outer atmosphere, Pennsylvania State University Ionos. Res. Lab. Sci. Rept. No. 69, 1954.
- Dungey, J.W., Hydromagnetic waves, in *Physics of Geomagnetic Phenomena*, edited by S. Matsushita and W.H. Campbell, vol. 2, Academic, San Diego, Calif., pp. 913-934, 1967.
- Elkington, S.R., M.K. Hudson, and A.A. Chan, Resonant acceleration and diffusion of outer zone electrons in an asymmetric geomagnetic field, *J. Geophys. Res.*, 108, doi:10.1029/2001JA009202, 2003.
- Elphinstone, R.D., J.S. Murphree, D.J. Hearn, L.L. Cogger, I. Sandahl, P.T. Newell, D.M. Klumpar, S. Ohtani, J.A. Sauvaud, T.A. Potemra, K. Mursula, A.N. Wright, and M. Shapshak, The double oval UV auroral distribution: 2. The most poleward arc system and the dynamics of the magnetotail, *J. Geophys. Res.*, 100, 12093, 1995.
- Engebretson, M., K.-H. Glassmeier, M. Stellmacher, W.J. Hughes, and H. Luhr, The dependence of high-latitude Pc5 wave power on solar wind velocity and on the phase of high speed solar wind streams, *J. Geophys. Res.*, 103, 26,271, 1998.
- Fenrich, F.R., J.C. Samson, G. Sofko, and R.A. Greenwald, ULF high- and low-*m* field line resonances observed with the Super Dual Auroral Radar Network, *J. Geophys. Res.*, 100, 21,535, 1995.
- Freeman, M.P., Effect of magnetopause leakage on the lifetime of magnetospheric cavity modes, *J. Geophys. Res.*, 105, 5463, 2000.
- Friedel, R.H.W., G.D. Reeves, and T. Obara, Relativistic electron dynamics in the inner magnetosphere: A review, *J. Atmos. Sol. Terr. Phys.*, 64, 265, 2002.
- Greenwald, R.A., and A.D.M. Walker, Energetics of long period resonant hydromagnetic waves, *Geophys. Res. Lett.*, 7, 745, 1980.
- Harrold, B.G., and J.C. Samson, Standing ULF modes of the magnetosphere: A theory, *Geophys. Res. Lett.*, 19, 1811, 1992.
- Hasegawa, A., K.H. Tsui, and A.S. Asis, A theory of long period magnetic pulsations. III - Local field line oscillations, *Geophys. Res. Lett.*, 10, 765, 1983.

- Hughes, W.J., Magnetospheric ULF waves: A tutorial with a historical perspective, in *Solar Wind Sources of Magnetospheric Ultra-Low-Frequency Waves*, *Geophys. Monogr. Ser.*, 81, edited by M.J. Engebretson, K. Takahashi, and M. Scholer, p1, AGU, Washington, D.C., 1994.
- Keiling, A., J.R. Wygant, C. Cattell, W. Peria, G. Parks, M. Temerin, F.S. Moser, C.T. Russell, and C.A. Kletzing, Correlation of Alfvén wave Poynting flux in the plasma sheet at 4-7 R_E with ionospheric electron energy flux, *J. Geophys. Res.*, 107, doi:10.1029/2001JA900140, 2002.
- Keiling, A. *et al.*, Some properties of Alfvén waves: Observations in the tail lobes and plasma sheet boundary layer, *J. Geophys. Res.*, *in press*, 2005.
- Kepko, L., H.E. Spence, and H.J. Singer, ULF waves in the solar wind as direct drivers of magnetospheric pulsations, *Geophys. Res. Lett.*, 29 (8), doi:10.1029/2001GL014405, 2002.
- Kivelson, M.G., J. Etcheto, and J.G. Trotignon, Global compressional oscillations of the terrestrial magnetosphere: The evidence and a model, *J. Geophys. Res.*, 89, 9851, 1984.
- Kivelson, M.G., and D.J. Southwood, Resonant ULF waves: A new interpretation, *Geophys. Res. Lett.*, 12, 49, 1985.
- Kivelson, M.G., and D.J. Southwood, Coupling of global magnetospheric MHD eigenmodes to field line resonances, *J. Geophys. Res.*, 91, 4345, 1986.
- Knight, S., Parallel electric fields, *Planet. Space Sci.*, 21, 741, 1973.
- Kouznetsov, I., and W. Lotko, Radial energy transport by magnetospheric ULF waves: Effects of magnetic curvature and plasma pressure, *J. Geophys. Res.*, 100, 7599, 1995.
- Landau, L.D., and E.M. Lifshitz, *Fluid Mechanics*, Pergamon, Oxford, 1987.
- Lee, D.H., and R.L. Lysak, Magnetospheric ULF wave coupling in the dipole model: the impulsive excitation, *J. Geophys. Res.*, 94, 17,097, 1989.
- Lee, D.-H., M.K. Hudson, K. Kim, R.L. Lysak, and Y. Song, Compressional MHD wave transport in the magnetosphere 1. Reflection and transmission across the plasmopause, *J. Geophys. Res.*, 107, doi:10.1029/2002JA009239, 2002.
- Liu, W.W., B.-L. Xu, J.C. Samson, and G. Rostoker, Theory and observations of auroral substorms: A magnetohydrodynamic approach, *J. Geophys. Res.*, 100, 79, 1995.
- Lühr, H., The IMAGE Magnetometer Network, *STEP Int.*, 4, pp. 4-6, 1994.
- Lyons, L.R., *et al.*, Auroral poleward boundary intensifications and tail bursty flows: A manifestation of a large-scale ULF oscillation?, *J. Geophys. Res.*, 107, 1352, doi:10.1029/2001JA000242, 2002.
- Mann, I.R., A.N. Wright, and P.S. Cally, Coupling of magnetospheric cavity modes to field line resonances: A study of resonance widths, *J. Geophys. Res.*, 104, 100, 19,441, 1995.
- Mann, I.R., A.N. Wright, and A.W. Hood, Multiple-timescales analysis of ideal poloidal Alfvén waves, *J. Geophys. Res.*, 102, 2381, 1997.
- Mann, I.R., G. Chisham, and S.D. Bale, Multisatellite and ground-based observations of a tailward propagating Pc5 magnetospheric waveguide mode, *J. Geophys. Res.*, 102, 4657, 1997.
- Mann, I.R., On the internal radial structure of field line resonances, *J. Geophys. Res.*, 102, 27,109, 1997.
- Mann, I.R. and A.N. Wright, Diagnosing the excitation mechanisms of Pc5 magnetospheric flank waveguide mode and FLRs, *Geophys. Res. Lett.*, 26, 2609, 1999.
- Mann, I.R., A.N. Wright, K.J. Mills, and V.M. Nakariakov, Excitation of magnetospheric waveguide modes by magnetosheath flows, *J. Geophys. Res.*, 104, 333, 1999.
- Mann, I.R., I. Voronkov, M. Dunlop, E.F. Donovan, T.K. Yeoman, D.K. Milling, J. Wild, K. Kauristie, O. Amm, S.D. Bale, A. Balogh, A. Viljanen, and H.J. Opgenoorth, Co-ordinated ground-based and Cluster observations of large amplitude global magnetospheric oscillations during a fast solar wind speed interval, *Ann. Geophys.*, 20, 405, 2002.
- Mann, I.R., T.P. O'Brien, and D.K. Milling, Correlations between ULF power, solar wind speed, and relativistic electron flux in the magnetosphere: Solar cycle dependence, *J. Atmos. Sol. Terr. Phys.*, 66, 187, 2004.
- Manuel, J.R., and J.C. Samson, The spatial development of the low-latitude boundary layer, *J. Geophys. Res.*, 98, 17,367, 1993.
- Mathews, J.T., I.R. Mann, I.J. Rae, and J. Moen, Multi-instrument observations of ULF wave-driven discrete auroral arcs propagating sunward and equatorward from the poleward boundary of the duskside auroral oval, *Phys. Plasmas*, 11, 1250, 2004.
- Mathews, J.T., The Role of ULF Waves in Energy Transport in the Magnetosphere, *Ph.D Thesis*, University of Alberta, 2005.
- Mathie, R.A., I.R. Mann, F.W. Menk, and D. Orr, Pc5 ULF pulsations associated with waveguide modes observed with the IMAGE magnetometer array, *J. Geophys. Res.*, 104, 7025, 1999a.
- Mathie, R.A., F.W. Menk, I.R. Mann, and D. Orr, Discrete field line resonances and the Alfvén continuum in the outer magnetosphere, *Geophys. Res. Lett.*, 26, 659, 1999b.
- Mathie, R.A., and I.R. Mann, Observations of Pc5 field line resonance azimuthal phase speeds: A diagnostic of their excitation mechanism, *J. Geophys. Res.*, 105, 10,713, 2000a.
- Mathie, R.A., and I.R. Mann, A correlation between extended intervals of ULF wave power and storm-time geosynchronous relativistic electron flux enhancements, *Geophys. Res. Lett.*, 27, 3261, 2000b.
- Mathie, R.A., and I.R. Mann, On the solar wind control of Pc5 ULF pulsation power at mid-latitudes: Implications for MeV electron acceleration in the outer radiation belt, *J. Geophys. Res.*, 106, 29,783, 2001.
- McDiarmid, D.R., A.N. Wright, and W. Allan, Time-limited excitation of damped field-line resonances: Implications for satellite observations, *J. Geophys. Res.*, 104, 17,409, 1999.
- McKenzie, J.F., Hydromagnetic wave interaction with the magnetopause and the bow shock, *Planet. Space Sci.*, 18, 1, 1970.
- Milling, D.K., I.R. Mann, and F.W. Menk, Diagnosing the plasmopause with a network of closely spaced ground-based magnetometers, *Geophys. Res. Lett.*, 28, 115, 2001.
- Mills, K.J., and A.N. Wright, Azimuthal phase speeds of FLRs driven by Kelvin-Helmholtz unstable waveguide modes, *J. Geophys. Res.*, 104, 22,667, 1999.
- Mills, K.J., A.N. Wright, and I.R. Mann, Kelvin-Helmholtz driven modes of the magnetosphere, *Phys. Plasmas*, 6, 4070, 1999.
- Mills, K.J., A.W. Longbottom, A.N. Wright and M.S. Ruderman, The Kelvin-Helmholtz instability of the magnetospheric flanks - An absolute and convective instability approach, *J. Geophys. Res.*, 105, 27,685, 2000.
- Mills, K.J., and A.N. Wright, Trapping and excitation of modes in the magnetotail, *Phys. Plasmas*, 7, 1572, 2000.
- Newton, R.S., D.J. Southwood, and W.J. Hughes, Damping of geomagnetic pulsations by the ionosphere, *Planet. Space Sci.*, 26, 201, 1978.
- Nielsen, E., and W. Allan, A double-resonance Pc-5 pulsation, *J. Geophys. Res.*, 88, 5760, 1983.
- O'Brien, T.P., K. Lorentzen, I.R. Mann, N.P. Meredith, J.B. Blake, J.F. Fennell, M.D. Looper, D.K. Milling, R.R. Anderson, Energization of relativistic electrons in the presence of ULF power and MeV microbursts: Evidence for dual ULF and VLF acceleration, *J. Geophys. Res.*, 108, 1329, doi:10.1029/2002JA009784, 2003.
- Prikryl, P., J.W. MacDougall, I.F. Grant, D.P. Steele, G.J. Sofko, and R.A. Greenwald, Observations of polar patches generated by solar wind Alfvén wave coupling to the dayside magnetosphere, *Ann. Geophys.*, 17, 463, 1999.
- Radoski, H.R., Highly asymmetric MHD resonances: The guided poloidal mode, *J. Geophys. Res.*, 72, 4026, 1967.
- Rae, I.J., E.F. Donovan, I.R. Mann, F. Fenrich, C. Watt, D.K. Milling, M. Lester, B. Lavraud, J. Wild, H.J. Singer, H. Reme, and A. Balogh, Evolution and characteristics of global Pc5 ULF waves during a high solar wind speed interval, *J. Geophys. Res.*, *in press*, 2005.
- Rae, I.J., I.R. Mann, E.F. Donovan, and E. Spanswick, Multiple field line resonances: Optical, magnetic, and absorption signatures, *Planet. Space Sci.*, *Submitted*, 2005.
- Rankin, R., J.C. Samson, and V.T. Tikhonchuk, Parallel electric fields in dispersive shear Alfvén waves, *Geophys. Res. Lett.*, 26, 3601, 1999.
- Rankin, R., K. Kabin, J.Y. Lu, I.R. Mann, R. Marchand, I.J. Rae, V.T. Tikhonchuk, and E.F. Donovan, Magnetospheric field-line resonances: Ground-based observations and modelling, *J. Geophys. Res.*, 110, doi:10.1029/2004JA010919, 2005.
- Rickard, G.J., and A.N. Wright, Alfvén resonance excitation and fast wave propagation in magnetospheric waveguides, *J. Geophys. Res.*, 99, 13455, 1994.
- Rickard, G.J., and A.N. Wright, ULF pulsations in a magnetospheric waveguide: Comparison of real and simulated satellite data, *J. Geophys. Res.*, 100, 3531, 1995.

- Rönmark, K., Electron acceleration in the auroral current circuit, *Geophys. Res. Lett.*, 26, 983, 1999.
- Rostoker, G., S. Skone, and D.N. Baker, On the origin of relativistic electrons in the magnetosphere associated with some geomagnetic storms, *Geophys. Res. Lett.*, 25, 3701, 1998.
- Ruohoniemi, J.M., R.A. Greenwald, K.B. Baker, and J.C. Samson, HF radar observations of Pc5 field line resonances in the midnight/early morning MLT sector, *J. Geophys. Res.*, 96, 15,697, 1991.
- Samson, J.C., J.A. Jacobs, and G. Rostoker, Latitude-dependent characteristics of long-period geomagnetic pulsations, *J. Geophys. Res.*, 76, 3675, 1971.
- Samson, J.C., R.A. Greenwald, J.M. Ruohoniemi, T.J. Hughes, and D.D. Wallis, Magnetometer and radar observations of magnetohydrodynamic cavity modes in the earth's magnetosphere, *Can. J. Phys.*, 69, 929, 1991a.
- Samson, J.C., T.J. Hughes, F. Creutzberg, D.D. Wallis, R.A. Greenwald, and J.M. Ruohoniemi, Observations of a detached, discrete arc in association with field line resonances, *J. Geophys. Res.*, 96, 15,683, 1991b.
- Samson, J.C., D.D. Wallis, T.J. Hughes, T.J. Creutzberg, J.M. Ruohoniemi, and R.A. Greenwald, Substorm intensifications and field line resonances in the nightside magnetosphere, *J. Geophys. Res.*, 97, 8495, 1992a.
- Samson, J.C., B.G. Harrold, J.M. Ruohoniemi and A.D.M. Walker, Field line resonances associated with MHD waveguides in the magnetosphere, *Geophys. Res. Lett.*, 19, 441, 1992b.
- Samson, J.C., L.L. Cogger, and Q. Pao, Observations of field line resonances, auroral arcs, and auroral vortex structures, *J. Geophys. Res.*, 101, 17,373, 1996.
- Scoffield, H.C., T.K. Yeoman, D.M. Wright, S.E. Milan, A.N. Wright, R.J. Strangeway, An investigation of the field aligned currents associated with a large scale ULF wave using data from CUTLASS and FAST, *Ann. Geophysicae*, 23, 487, 2005.
- Southwood, D.J., Some features of field line resonances in the magnetosphere, *Planet. Space Sci.*, 22, 483, 1974.
- Southwood, D.J., and W.J. Hughes, Theory of hydromagnetic waves in the magnetosphere, *Space Sci. Rev.*, 35, 301, 1983.
- Southwood, D.J., and M.G. Kivelson, The magnetohydrodynamic response of the magnetospheric cavity to changes in solar wind pressure, *J. Geophys. Res.*, 95, 2301, 1990.
- Stephenson, J.A.E., A.D.M. Walker, HF radar observations of Pc5 ULF pulsations driven by the solar wind, *Geophys. Res. Lett.*, 29, doi:10.1029/2001GL014291, 2002.
- Streltsov, A., and W. Lotko, Dispersive, nonradiative field line resonances in a dipolar magnetic field geometry, *J. Geophys. Res.*, 102, 27,121, 1997.
- Streltsov, A.V., W. Lotko, J.R. Johnson, C.Z. Cheng, Small-scale, dispersive field line resonances in the hot magnetospheric plasma, *J. Geophys. Res.*, 103, 26,559, 1998.
- Takahashi, K., S. Ohtani, W.J. Hughes, R.R. Anderson, CRRES observation of Pi2 pulsations: Wave mode inside and outside the plasmasphere, *J. Geophys. Res.*, 106, 15,567, 2001.
- Vaivads, A. *et al.*, What high altitude observations tell us about the auroral acceleration: A Cluster/DMSPP conjunction, *Geophys. Res. Lett.*, 30 (3), 1106, doi:10.1029/2002GL016006, 2003.
- Vedin, J., and K. Rönmark, Electron pressure effects on driven auroral Alfvén waves, *J. Geophys. Res.*, 110, A01214, doi:10.1029/2004JA010610, 2005.
- Vennerström, S., Dayside magnetic ULF power at high latitudes: A possible long-term proxy for the solar wind velocity?, *J. Geophys. Res.*, 104, 10,145, 1999.
- Villante, U., P. Francia, and S. Lepidi, Pc5 geomagnetic field fluctuations at discrete frequencies at a low-latitude station, *Ann. Geophys.*, 19, 321, 2001.
- Walker, A.D.M., R.A. Greenwald, W.F. Stuart, and C.A. Green, Stare auroral radar observations of Pc5 geomagnetic pulsations, *J. Geophys. Res.*, 84, 3373, 1979.
- Walker, A.D.M., The Kelvin-Helmholtz instability in the low-latitude boundary layer, *Planet. Space Sci.*, 29, 1119, 1981.
- Walker, A.D.M., J.M. Ruohoniemi, K.B. Baker, R.A. Greenwald and J.C. Samson, Spatial and temporal behaviour of ULF pulsations observed by the Goose Bay HF radar, *J. Geophys. Res.*, 97, 12187, 1992.
- Walker, A.D.M., Excitation of magnetohydrodynamic cavities in the magnetosphere, *J. Atmos. Solar-Terr. Phys.*, 60, 1279, 1998.
- Walker, A.D.M., Excitation of field line resonances by MHD waves originating in the solar wind, *J. Geophys. Res.*, 107, doi:10.1029/2001JA009188, 2002.
- Walker, A.D.M., Magnetohydrodynamic Waves in Geospace: The Theory of ULF Waves and Their Interaction with Energetic Particles in the Solar-Terrestrial Environment, Institute of Physics, London, 2004.
- Wanliss, J.A., R. Rankin, J.C. Samson, and V.T. Tikhonchuk, Field line resonances in a stretched magnetotail: CANOPUS optical and magnetometer observations, *J. Geophys. Res.*, 107, doi:10.1029/2001JA000257, 2002.
- Waters, C.L., and J.C. Samson, and E.F. Donovan, Variation of plasmatrough density derived from magnetospheric field line resonances, *J. Geophys. Res.*, 101, 24,737, 1996.
- Watt, C.E.J., R. Rankin, and R. Marchand, Kinetic simulations of electron response to shear Alfvén waves in magnetospheric plasmas, *Phys. Plasmas*, 11, doi:10.1063/1.1647140, 2004.
- Wright, A.N., Asymptotic and time-dependent solutions of magnetic pulsations in realistic magnetic field geometries, *J. Geophys. Res.*, 97, 6439, 1992.
- Wright, A.N., Dispersion and wave coupling in inhomogeneous MHD waveguides, *J. Geophys. Res.*, 99, 159, 1994.
- Wright, A.N., Energy sources of field-aligned currents: Auroral electron energization, *J. Geophys. Res.*, 110, A10S08, doi:10.1029/2004JA010609, 2005.
- Wright, A.N., and W. Allan, Structure, phase motion, and heating within Alfvén resonances, *J. Geophys. Res.*, 101, 17,399, 1996.
- Wright, A.N., W. Allan, and P.A. Damiano, Alfvén wave dissipation via electron energization, *Geophys. Res. Lett.*, 30 (16) 1847, doi:10.1029/2003GL017605, 2003.
- Wright, A.N., W. Allan, R.D. Elphinstone, and L.L. Cogger, Phase mixing and phase motion of Alfvén waves on tail-like and dipole-like magnetic field lines, *J. Geophys. Res.*, 104, 10,159, 1999.
- Wright, A.N., W. Allan, M.R. Ruderman, and R.C. Elphic, The dynamics of current carriers in standing Alfvén waves: Parallel electric fields in the auroral acceleration region, *J. Geophys. Res.*, 107 (A7), doi:10.1029/2001JA900168, 2002.
- Wright, A.N., and A.W. Hood, Field-aligned electron acceleration in Alfvén waves, *J. Geophys. Res.*, 108 (A3), 1135, doi:10.1029/2002JA009551, 2003.
- Wright, A.N., K.J. Mills, A.W. Longbottom, and M.S. Ruderman, The nature of convectively unstable waveguide mode disturbances on the magnetospheric flanks, *J. Geophys. Res.*, 107, 1242, doi:10.1029/2000JA005091, 2002.
- Wright, A.N., K.J. Mills, M.S. Ruderman, and L. Brevdo, The absolute and convective instability of the magnetospheric flanks, *J. Geophys. Res.*, 105, 385, 2000.
- Wright, A.N., and G.J. Rickard, ULF pulsations driven by magnetopause motions: Azimuthal phase characteristics, *J. Geophys. Res.*, 100, 23,703, 1995.
- Wright, A.N., and M.J. Thompson, Analytical treatment of Alfvén resonances and singularities in nonuniform magnetoplasmas, *Phys. Plasmas*, 1, 691, 1994.
- Wygant *et al.*, Polar spacecraft based comparison of intense electric fields and Poynting flux near and within the plasma sheet-tail lobe boundary to UVI images: An energy source for the aurora, *J. Geophys. Res.*, 105, 18,675, 2000.
- Zhu, X., and M.G. Kivelson, Analytic formulation and quantitative solutions of the coupled ULF problem, *J. Geophys. Res.*, 94, 8602, 1988.
- Ziesolleck, C.W.S., and D.R. McDiarmid, Auroral latitude Pc5 field line resonances: Quantized frequencies, spatial characteristics, and diurnal variation, *J. Geophys. Res.*, 99, 5817, 1994.

I.R. Mann, Department of Physics, University of Alberta, Edmonton, Alberta T6G 2J1, Canada. (imann@phys.ualberta.ca)

A.N. Wright, Mathematical Institute, University of St. Andrews, St. Andrews, Fife KY16 9SS, UK. (andy@mcs.st-and.ac.uk)